28

Creation of a Biopacemaker: Lessons from the Sinoatrial Node

A. Dénise den Haan, Arie O. Verkerk and Hanno L. Tan
Heart Failure Research Center, University of Amsterdam, Amsterdam
The Netherlands

1. Introduction

The sinoatrial (SA) node is the normal pacemaker of the mammalian heart and generates the electrical impulse for the regular, rhythmic contraction of the heart. SA node dysfunction and high-grade atrioventricular block may lead to failing impulse generation or propagation towards the ventricles. The resulting bradycardia may be life-threatening and is currently treated with implantation of an electronic pacemaker. Shortcomings of this technique include limited autonomic responsiveness, suboptimal cardiac activation pathways, limited battery life, magnetic interference, and risk of infections. In order to avoid these drawbacks research has focused on the development of genetically engineered biological pacemakers (biopacemakers).

To date, various approaches have been used to create biopacemakers. However, the biopacemaker in its current state is not applicable in humans. Before biopacemakers may find their way to the bedside, various issues need to be resolved for long-term function, including the ratio between upregulated inward currents and downregulated outward currents, the optimal site in the heart for genetic modification or implantation, optimal cell mass, and optimal electrical coupling to surrounding tissues.

A logical approach to improve the biopacemaker would be to implement our knowledge about the way in which the physiological pacemaker, the SA node, functions. In this chapter, we focus on function, structure, and regulation of the SA node in relation to the creation of a biopacemaker.

2. Ionic currents in the SA node

The action potential of SA nodal myocytes differs from that found in atrial or ventricular cells. Firstly, there is a slow diastolic depolarization (phase 4 depolarization), where cells depolarize spontaneously towards the action potential threshold. Secondly, the action potential upstroke (phase 0) is slow compared to the upstroke in atrial and ventricular myocytes. Thirdly, SA node cells have a less negative maximal diastolic potential (MDP).

The SA node action potential is a result of a complex interaction of multiple inwardly and outwardly directed ion currents, which are summarized in Figure 1 (for reviews see Boyett et al., 2000; Dobrzynski et al., 2007; Irisawa et al., 1993; Mangoni & Nargeot, 2008).

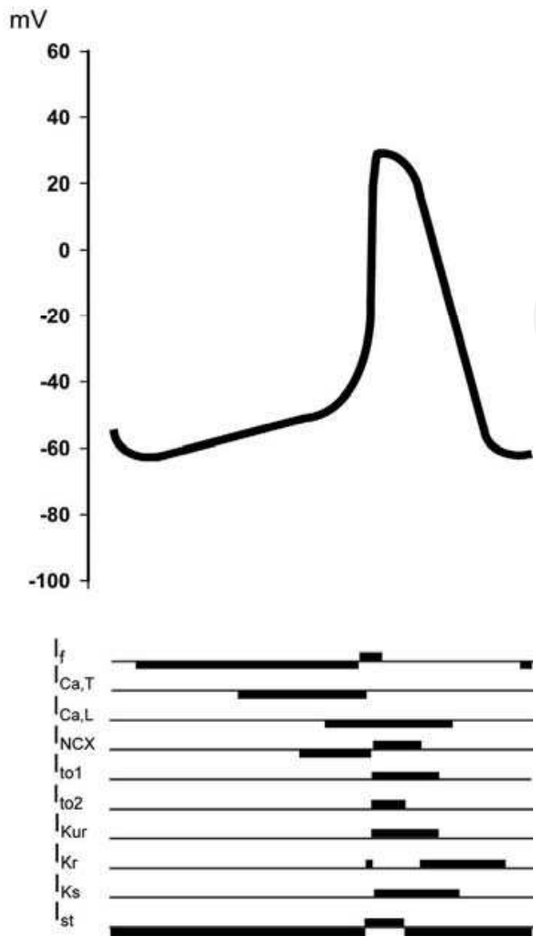

Downward bars indicate inward currents, upward bars outward currents. I_f = hyperpolarisation-activated current; $I_{Ca,T}$ = transient type Ca^{2+} current; $I_{Ca,L}$ = long lasting Ca^{2+} current; I_{NCX} = Na^+-Ca^{2+} exchange current; I_{to1} = transient outward current type 1; I_{to2} = transient outward current type 2; I_{Kur} = ultra-rapid component of the delayed rectifier current; I_{Kr} = rapid component of the delayed rectifier current; I_{Ks} = slow component of the delayed rectifier current; I_{st} = sustained inward current.

Fig. 1. SA node myocytes action potential and ionic currents.

2.1 Hyperpolarization-activated current (funny current, I_f)

Before the discovery of the hyperpolarization-activated current, the diastolic depolarization was thought to result from the decay of an outward K^+ current (Noble & Tsien, 1968). However, in 1979 this decaying outward current was shown to be an inward current activated upon hyperpolarization (Brown et al., 1979). Figure 2A, left panel, shows a typical example of the hyperpolarization-activated current in a rabbit SA node cell. Due to its activation upon hyperpolarization and mixed permeability to Na^+ and K^+, this current was named the funny current (I_f). The voltage-gated ion channels responsible for I_f are encoded by four gene isoforms: *HCN1* through *HCN4* (Ludwig et al., 1998; Stieber et al., 2004). All of these are found in the heart, with *HCN4* mRNA being most prevalent in human (Chandler et al., 2009) and rabbit SA node (Brioschi et al., 2009; Chandler et al., 2009). The physiological relevance of there being multiple isoforms may lie in their distinct kinetics and their

different responsiveness to autonomic stimulation, with half-maximal activation voltages being more negative for *HCN4* than for *HCN2*, and *HCN4* having a larger increase in rate of activation in the presence of cAMP (Verkerk et al., 2009a). However, none of these isoforms seem to be capable of forming homomers that have properties corresponding to those of native I_f in rabbit SA node cells (Altomare et al., 2003) or (neonatal) rat ventricular cells (Qu et al., 2002; Qu et al., 2001). This led to the hypothesis that different isoforms could form heteromers with intermediate characteristics. By both expressing *HCN1* and *HCN2* in equal amounts, and by expressing a concatenated *HCN1-HCN2* construct, Ulens and Tytgat provided evidence that these subunits could spontaneously form heteromeric subunits (Jackson et al., 2007; Ulens & Tytgat, 2001).

In human SA node cells, I_f activates at potentials negative to –50 mV, with a reversal potential of -22.1±2.4 mV, due to its mixed permeability to both Na^+ and K^+ (Verkerk et al., 2007a). In rabbit SA node cells, I_f was found to reverse around -24 mV with a half-maximal activation at -76.1 mV (van Ginneken & Giles, 1991). Figure 2A, right panel, shows the average current-voltage (I-V) relationship of I_f in rabbit SA node cells during hyperpolarization (I_{step}) and upon stepping back to the holding potential of –40 mV (I_{tail}). I_{tail} is used to analyze the voltage dependency of current activation. The speed of activation and the voltage dependency of activation of HCN channels is influenced by a variety of factors (for review see Verkerk et al., 2009a), including both sympathetic and parasympathetic stimulation (Baruscotti et al., 2005). Direct interaction of cAMP with the cyclic nucleotide binding domain of HCN shifts the voltage dependence of activation towards more depolarized potentials (Wainger et al., 2001) and speeds up current activation. Furthermore, increased phosphorylation can cause an increase in I_f by increasing maximal conductance in a voltage independent way, and by increasing sensitivity to β-adrenergic stimulation (Accili et al., 1997).

Qu et al. showed that the kinetics of I_f are also context dependent with a less negative threshold of activation for *HCN2* and *HCN4* in neonatal ventricular myocytes than in HEK 293 cells (Qu et al., 2002). Factors possibly regulating I_f are auxiliary subunits (Decher et al., 2003) and cellular characteristics (Barbuti et al., 2004).

Properties that make I_f a likely current to be responsible for automaticity include the initiation of an inward current during diastolic, hyperpolarized potentials, its sensitivity to autonomous modulation, and its presence in pacemaking cells. However, due to other properties the role of I_f in cardiac automaticity remains a matter of debate (see Verkerk et al., 2009a and primary refs cited therein). The continuing debate on the physiological significance of I_f in SA node pacemaking is strongly related to the intrinsically slow activation kinetics and negative activation profile of I_f relative to the time scale and the voltage range of diastolic depolarization in the SA node. Other arguments are the fact that even though blocking I_f with drugs decreases beating rate, it does not completely block spontaneous activity, and that conditional *HCN4* knock out mice still show sinus rhythm (for review see Lakatta & DiFrancesco, 2009).

2.2 Ca^{2+} currents

2.2.1 T-type Ca^{2+} current ($I_{Ca,T}$)

So far, three different genes have been found that encode transient type (T-type) Ca^{2+} channels: $Ca_v3.1$ through $Ca_v3.3$, encoded by *CACNA1G* through *CACNA1I* (Perez-Reyes, 1999). Both $Ca_v3.1$ and $Ca_v3.3$ mRNA were found in the human SA node, with $Ca_v3.1$

mRNA and protein being more prevalent in the SA node than right atrium (Chandler et al., 2009). However, in murine SA node, no $Ca_v3.3$ mRNA has been identified, while $Ca_v3.2$ is present (Bohn et al., 2000; Marionneau et al., 2005).

When first characterized in rabbit SA node, T-type Ca^{2+} current ($I_{Ca,T}$) was found to activate at -47±2.4 mV with a voltage of half maximal activation at -23 mV (Hagiwara et al., 1988). Figure 2B shows a typical example and I-V relationship of $I_{Ca,T}$ in rabbit SA node cells. However, overexpression of different subtypes of Cav3.x in HEK293 cells showed a more hyperpolarized activation threshold and more hyperpolarized half maximal activation values. Activation thresholds were found to be -70 mV for $Ca_v3.1$, -55 mV for $Ca_v3.2$, and -80 mV for $Ca_v3.3$, with voltages of half maximal activation of -51.73, -43.15, and -60.7 mV respectively (McRory et al., 2001).

While, at first, $I_{Ca,T}$ was thought to be insensitive to neuromediators, several neuromediators, including norepinephrine and phenylephrine, were found to influence $I_{Ca,T}$ (Vassort & Alvarez, 1994). These effects have been found in different cell types, while the only mediator investigated in SA node, isoproterenol, did not show any effect (Hagiwara et al., 1988).

Bean was the first to hypothesize about the role of $I_{Ca,T}$ in automaticity, suggesting that fast Ca^{2+} channels would be useful in cells capable of generating spontaneous activity, since they will be activated at negative potentials and will help depolarize the cells, while the Na^+ channels are inactivated due to their more hyperpolarized inactivation curve (Bean, 1985). Indeed, blocking $I_{Ca,T}$ with 40 μM Ni^{2+} was shown to have a negative chronotropic effect on rabbit SA node cells by slowing the late phase of the diastolic depolarization (Hagiwara et al., 1988). When blocking $I_{Ca,T}$ specifically with R-efonidipine, this finding could not be reproduced completely, as this led to a clear increase in cycle length in mice, but not in rabbit (Tanaka et al., 2008).

The role of $I_{Ca,T}$ in murine SA node automaticity was confirmed in vivo by a slowing of mean heart rate in $Ca_v3.1^{-/-}$ mice, associated with a decrease in $I_{Ca,T}$. Patch clamp experiments of SA node cells of these mice showed a decrease in $I_{Ca,T}$, 37% slowing in cellular beating rate, and a decrease in depolarization slope of 44% (Mangoni et al., 2006). Since $Ca_v3.2$ was shown not to activate at voltages negative to -55 mV, with a voltage of half maximal activation of -43.15 (McRory et al., 2001), a considerable role in diastolic depolarization is not to be expected. Knock-out of $Ca_v3.2$, as predicted, had no significant effect on heart rate (Chen et al., 2003). This is also in agreement with SA node gene expression studies that show a higher level of $Ca_v3.1$ mRNA in SA node than other regions of the heart, but no difference in level of $Ca_v3.2$ mRNA (Chandler et al., 2009; Marionneau et al., 2005).

2.2.2 L-type Ca^{2+}current ($I_{Ca,L}$)

The cardiac long lasting type (L-type) Ca^{2+} channel consists of different subunits: α1-, β-, and α2-δ (Benitah et al., 2010). The α1-subunit forms the ion pore, and is selective for Ca^{2+} due to a high affinity binding site for Ca^{2+} within the pore (Yang et al., 1993). Different genes encode for different isoforms of the α1-subunit, with Cav1.2 (*CACNA1C*) and Cav1.3 (*CACNA1D*) mRNA being present in the human SA node. While Cav1.2 mRNA is more prevalent in atrial and nodal tissue, Cav1.3 is the only subtype more prevalent in SA node tissue than in atrial tissue (Chandler et al., 2009; Marionneau et al., 2005). When overexpressed in combination with a β-subunit, Cav1.3 channels were shown to activate at

more hyperpolarized membrane potentials (-55 mV versus –35 mV), and were less sensitive to dihydropyridines than Cav1.2 channels (Xu & Lipscombe, 2001).

Of the different β-subunits identified, Gao and coworkers only detected the β2-subunit in rabbit myocytes by immunoblotting (Gao et al., 1997). However, in human and canine ventricular tissue, Foell and colleagues demonstrated the presence of 18 different mRNA splice forms of all 4 β-subunit families (Foell et al., 2004). In human SA node, mRNA of the β2-, and, to a lesser extent, β1- and β3-subunits was found (Chandler et al., 2009). The function of β-subunits has partly been elucidated. Firstly, these subunits alter channel kinetics and voltage dependence (Benitah et al., 2010). Secondly β-subunits can bind to the part of the α1-subunit which is involved in retention to the endoplasmic reticulum, thereby relieving the inhibition of trafficking and thus causing increased channel incorporation into the cell membrane (Bichet et al., 2000). Furthermore, it was shown that an increase in cAMP is associated with an increase in phosphorylation of the β-subunit, while there is no change in phosphorylation of the α1-subunit. This implies that autonomic control of the L-type Ca2+ channel is regulated via the β-subunit (Haase et al., 1993). By overexpressing β1b, β2a, β3, and β4-subunits in adult rat ventricular myocytes, Colecraft and colleagues showed that different β-subunits have different functions. Overexpression of β2a and β4-subunits caused the biggest increase in current density and largest decrease in rate of inactivation. Cells overexpressing β2a showed predominant subunit localization to the cell membrane, while overexpression of β4-subnits showed staining of transverse elements and the nucleus (Colecraft et al., 2002).

The α_2-δ-subunit is a transmembrane subunit composed of 2 subunits encoded by the same gene, connected to each other by a disulfide bond (De Jongh et al., 1990). Singer and colleagues investigated the effect of the α_2-δ-subunit on the L-type Ca^{2+} current ($I_{Ca,L}$) by overexpression of different combinations of subunits in Xenopus oocytes (Singer et al., 1991). Addition of the α_2-δ subunit to the α_1-subunit resulted in an increase in current amplitude, sensitivity to the dihydropyridine agonist Bay K 8644, voltage sensitivity of inactivation, and faster activation.

The upstroke of the action potential in SA node cells depends on $I_{Ca,L.}$. Figure 2B shows a typical example of $I_{Ca,L}$ in rabbit SA node cells. Since one of the characteristics that distinguishes L-type Ca^{2+} channels from T-type Ca^{2+} channels is their opening at relatively depolarized potentials (Fig. 2B, right panel), their role in diastolic depolarization was long considered to be negligible. However, $Ca_v1.3$ opens at more hyperpolarized potentials than other isoforms (Xu & Lipscombe, 2001; Xue et al., 2002), and thus could play a more substantial role in automaticity. The difficulty in studying the importance of $I_{Ca,L}$ in diastolic depolarization lies in the fact that depolarization of SA node cells depends on this current, instead of the Na^+ current, and thus inhibition of $I_{Ca,L}$ will invariably influence automaticity. Verheijck and colleagues avoided this problem by applying a depolarizing pulse to rabbit SA node cells that had lost spontaneous activity due to 5 μM nifedipine, to a degree that subsequent repolarization and diastolic depolarization resembled those during spontaneous activity (Verheijck et al., 1999). This way, they showed that depolarization from a holding potential of -90 to –60 mV could already activate $I_{Ca,L.}$ Consequently this current could serve as an inward current during the entire diastolic depolarization. These findings were later confirmed in $Ca_v1.3$ knock out mice (Mangoni et al., 2003; Zhang et al., 2002b).

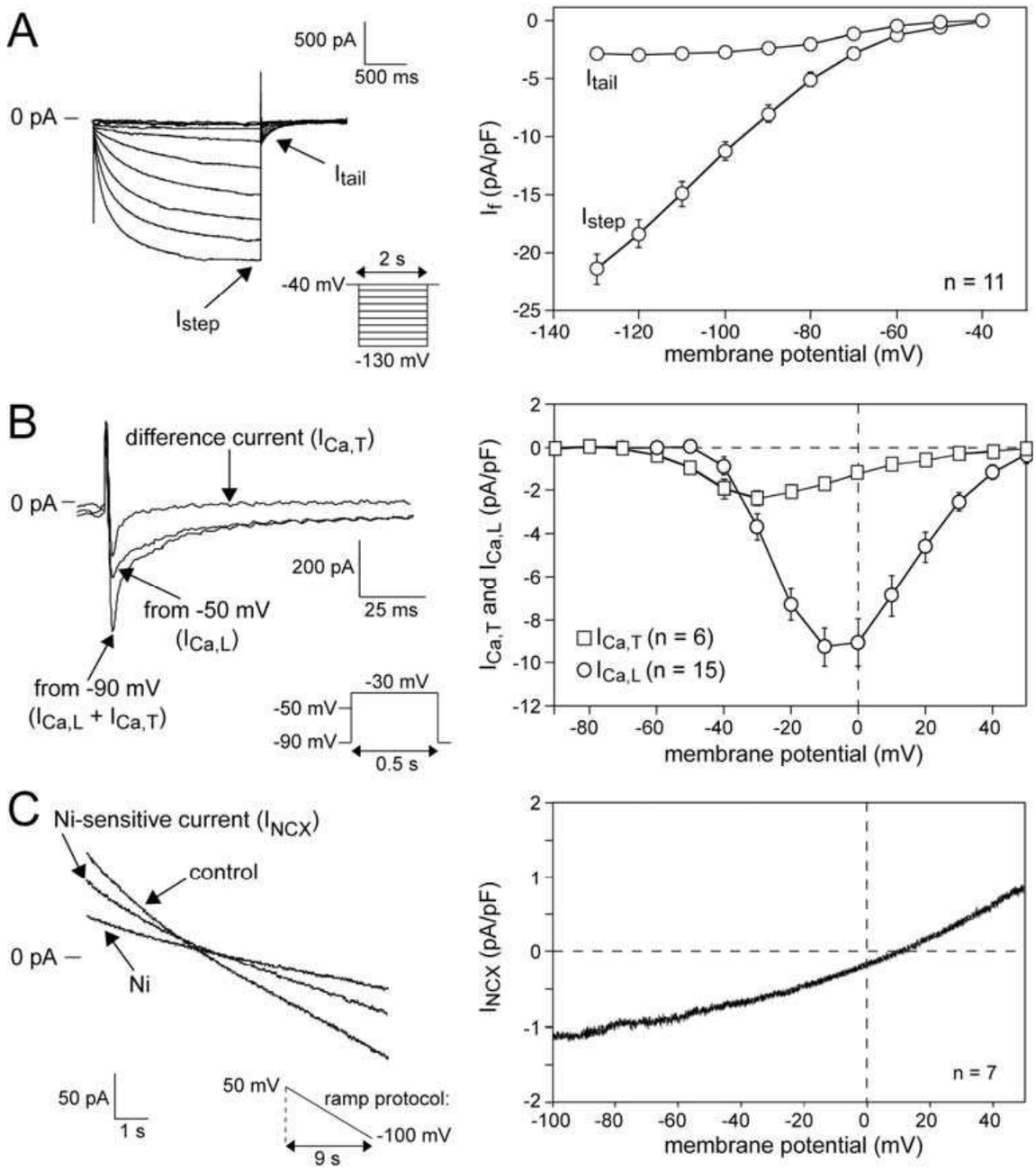

A, Typical examples (left) and average current-voltage (I-V) relation (right) of I_f. Inset, Voltage clamp protocol used. B, Typical examples (left) and average I-V (right) relation of $I_{Ca,T}$ and $I_{Ca,L}$. Inset, Voltage clamp protocol used. Please note that current traces were elicited by depolarizing voltage steps from -90 for combined measurements of $I_{Ca,L}$ and $I_{Ca,T}$ and -50 mV for measurements of only $I_{Ca,L}$. $I_{Ca,T}$, if present, was obtained as the difference current. C, Typical example (left) and average I-V relationship (right) of I_{NCX}. Inset, Voltage clamp protocol used. I_{NCX} was measured as Ni-sensitive current during a descending voltage clamp ramps. For cell isolations and experimental details, see Verkerk et al., 2003.

Fig. 2. Inward currents in rabbit SA node cells.

2.2.3 Ca^{2+} release activated Na^{+}-Ca^{2+} exchange current (I_{NCX})

In recent years, low-voltage activated Ca^{2+} releases (LVCRs) from the sarcoplasmic reticulum have attracted a lot of attention (for review see Lakatta et al., 2010). This Ca^{2+} release could increase the subsarcolemmal Ca^{2+} concentration, thereby activate the Na^{+}-Ca^{2+} exchanger (NCX) and thus generate an inward current (I_{NCX}) by extruding one Ca^{2+} in exchange for three Na^{+} (Blaustein & Lederer, 1999). In 1993 Zhou and colleagues showed that after activation of $I_{Ca,L,}$ there was a second inward current which was due to I_{NCX} (Zhou & Lipsius, 1993). Figure 2C shows a typical example and I-V relationship of I_{NCX} in rabbit SA node cells. This finding was further explored and led to a theory on spontaneous release from the sarcoplasmic reticulum as being the oscillator responsible for SA node automaticity (Maltsev et al., 2006). Conflicting evidence has been found regarding the spontaneous occurrence of these Ca^{2+} releases, with Huser and colleagues showing that LVCRs no longer occur when feline latent pacemaker cells are voltage clamped at a hyperpolarized resting potential (-70 mV), and only occur in the presence of depolarization, starting at a membrane potential of –57 mV. They also demonstrated that LVCRs depend on $I_{Ca,T}$, as they disappear when $I_{Ca,T}$ is blocked with 50 µM Ni^{+} (Huser et al., 2000). However, in rabbit SA node cells, addition of 50 µM Ni^{+} did not stop the occurrence of LVCRs, nor did voltage clamping these cells at -10 mV. At more negative holding potentials, LVCRs ceased due to a decrease in sarcoplasmic Ca^{2+} as a result of extrusion of Ca^{2+} following NCX activity after each Ca^{2+} release (Vinogradova et al., 2004).

2.3 Transient outward currents

2.3.1 Transient outward K^{+} current, type 1 (I_{to1})

Two transient outward current components are found in cardiac cells, one carried by K^{+} (I_{to1}), the other by Cl^{-} ions (I_{to2}) (Nerbonne & Kass, 2005). The pore-forming α-subunit of the transient outward K^{+} current I_{to1} is formed by different members of the Kv family. *KCND2* (Kv4.2) and *KCND3* (Kv4.3) encode $I_{to,fast}$, which recovers rapidly from inactivation, while *KCNA4* encodes Kv1.4, which recovers slowly from inactivation ($I_{to,slow}$) (Nerbonne & Kass, 2005). Similar to other channels from the Kv family, channels are formed by tetramerization. Multiple β-subunits have been proposed, including KChiPs (Kuo et al., 2001), MiRP1 (*KCNE2*) and MiRP2 (*KCNE3*) (Roepke et al., 2008; Zhang et al., 2001b), Kvβ (Aimond et al., 2005), and DPP6 (Radicke et al., 2005).

In human SA node, mRNA for Kv4.2, Kv1.4 and, in particular, Kv4.3 was found (Chandler et al., 2009); all these transcripts were also found in murine SA node (Marionneau et al., 2005).

Upon membrane depolarization, I_{to1} exhibits fast activation, followed by fast inactivation (Nerbonne & Kass, 2005). The influence of this current differs among different species and different parts of the heart. In ventricular tissue of most mammals, except for guinea pig (Sanguinetti & Jurkiewicz, 1990) and pig (Li et al., 2003), I_{to1} is responsible for the early phase of repolarization. Differences in I_{to1} density and composition between epicardium and endocardium may in part explain the difference in action potential waveform and duration in these different areas of the heart (Liu et al., 1993).

Investigation of the role of I_{to1} in SA node function is hampered by the lack of a specific blocker. In older studies 4-aminopyridine (4-AP) was used as a specific blocker for I_{to1} (Thompson, 1977). However, more recent studies have shown that 4-AP also blocks the

ultra-rapid, rapid, and slow components of the delayed rectifier K^+ current (I_{Kur}, I_{Kr}, and I_{Ks}, respectively) at concentrations used to analyze the role of I_{to1} (Li et al., 1996; Ridley et al., 2003; Arechiga-Figueroa et al., 2010). As will be discussed later, block of these currents influences SA node function. In addition, 4-AP stimulates $I_{K,Ach}$ (Arechiga-Figueroa et al., 2010).

Whether or not I_{to1} is present in SA node cells still remains to be resolved. The current was first described in cells from the crista terminalis of rabbit heart in 1985 (Giles & van Ginneken, 1985). This current was completely blocked by 4-AP, and activated between -20 and +10mV with a reversal potential around –75 mV. In 2000, Lei et al characterized the current in rabbit SA node (Lei et al., 2000). Using a holding potential of –80 mV and 200 ms pulses between -40 and 60 mV, they showed a rapidly activating (within 10 ms) current that inactivated within 200 ms, with a voltage of half maximal activation of -11 mV and a fast and a slow inactivating component (10 vs 107 ms). In the presence of an extremely high concentration of 4-AP (10 mM), the outward current was abolished. The effect of 4-AP on spontaneous activity of SA node cells was studied in small and large cells, under the assumption that small cells originate from the center of the SA node, while larger cells are situated more in the periphery. In small cells, 4-AP decreased action potential amplitude, increased action potential duration, decreased maximum diastolic potential, and increased cycle length. In large cells, spontaneous activity ceased. These observations seem to correspond with blockade of I_{Kur}, $I_{Kr,}$ and I_{Ks}, which are also blocked by 4-AP (see below). Based on these experiments, it is not possible to distinguish between the effects of these different currents.

In a letter to the editor based on this paper, Verkerk and Van Ginneken discuss the interference of I_f tail current when measuring I_{to1} (Verkerk & van Ginneken, 2001). Even in the presence of drugs that block I_f there will be interference due to the fact that these drugs will block the current more efficiently at hyperpolarized membrane potentials than during depolarization. In a study on ionic remodelling of SA node cells during heart failure by Verkerk et al., no I_{to1} was found to be present in rabbit SA node (Verkerk et al., 2003).

To our knowledge, no data have been published regarding the heart rate in genetically modified mice lacking I_{to1}.

2.3.2 Ca^{2+} activated Cl^- current ($I_{Cl(Ca)}$ or I_{to2})

In 2002 the Ca^{2+} activated Cl^- current ($I_{Cl(Ca)}$), also known as the 4-AP insensitive part of I_{to}, or I_{to2}, was found to be present in one third of spontaneously beating rabbit SA node cells (Verkerk 2002). Figure 3A, left panel, shows a typical example of $I_{Ca(Cl)}$ in rabbit SA node cells. This current, which is sensitive to 4,4,-diisothiocyanostilbene-2,2,-disulphonic acid (DIDS), is a transient outward current activated by Ca^{2+} release of the sarcoplasmic reticulum and is present at potentials positive to –20 mV with a peak at 40 mV (Fig. 3A, right panel). By decreasing $I_{Cl(Ca)}$, DIDS increased action potential overshoot and prolonged APD20, without affecting diastolic depolarization rate, MDP, action potential duration at 50% repolarization (APD_{50}), or cycle length. In the presence of norepinephrine, $I_{Cl(Ca)}$ density doubled, but also under these circumstances inhibition did not influence beating rate. Incorporation into in silico models of SA node cells also showed a limited role in pacemaker synchronization and conduction from SA node to atrium.

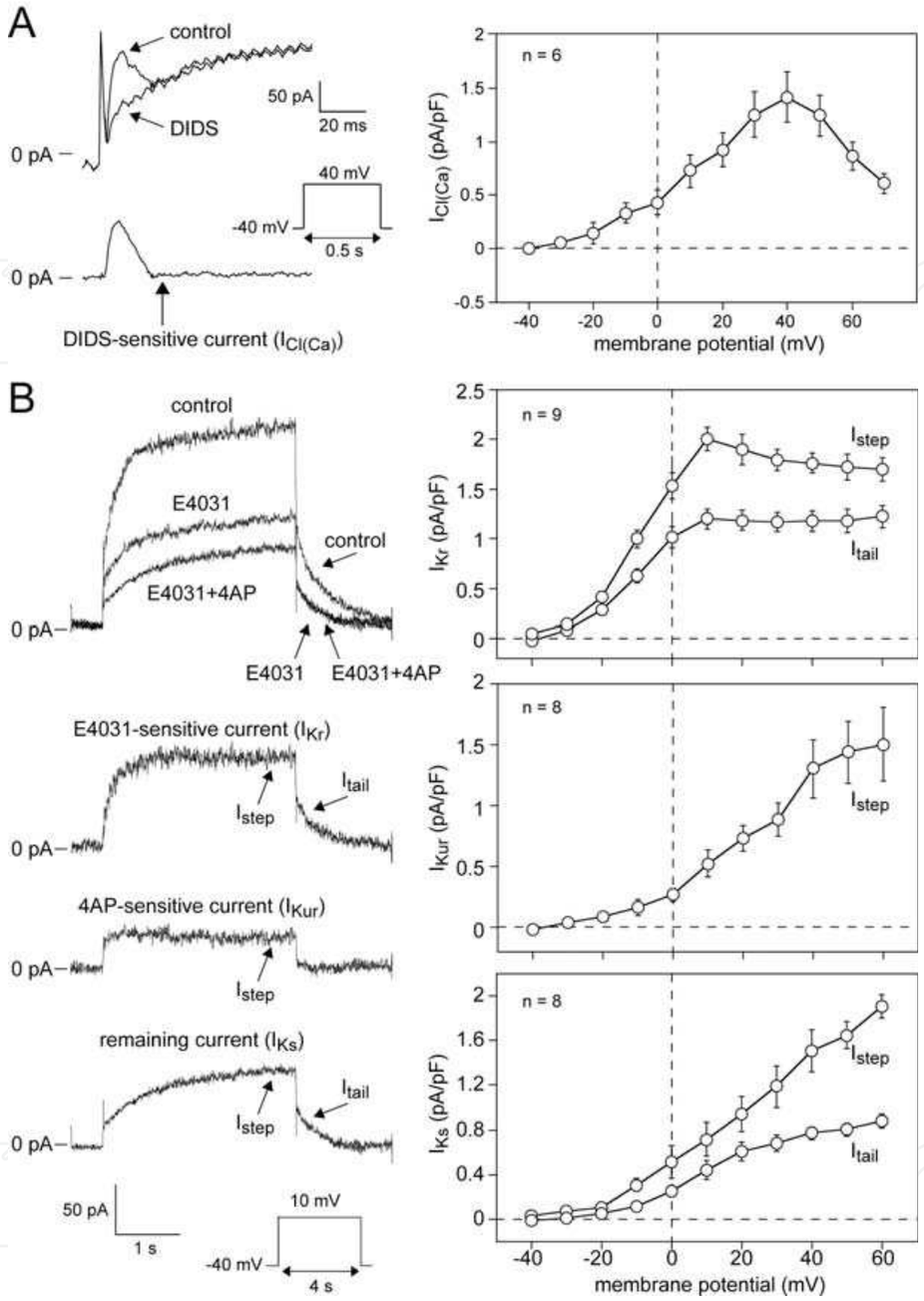

A, Typical example (left) and average I-V relationship (right) of the Ca^{2+}-activated Cl^- current ($I_{Cl(Ca)}$). Inset, Voltage clamp protocol used. $I_{Cl(Ca)}$ was measured as current sensitive for 4,4,-diisothiocyanostilbene-2,2,-disulphonic acid (DIDS) B, Typical examples (left) and average I-V relationships of the delayed rectifier K^+ currents (right). Inset, Voltage clamp protocol used. Currents were measured in control conditions, in presence of E4031 and in combined presence of E4031 and 4AP. E4031-sensitive current was defined as I_{Kr}, 4AP-sensitive current was defined as I_{Kur}, and remaining time-dependent current was defined as I_{Ks}. For cell isolations and experimental details, see Ref (Verkerk et al., 2003).

Fig. 3. Outward currents in rabbit SA node cells.

2.4 Delayed rectifier K^+ currents

The delayed rectifier K^+ current (I_K), first described in Purkinje fibers in 1968 (Noble & Tsien, 1968), is composed of three different components: the ultra-rapid (I_{Kur}), rapid (I_{Kr}), and slow (I_{Ks}) components. Figure 3B, shows typical examples and I-V relationships of the various I_K components in rabbit SA node cells. I_{Kur}, I_{Kr}, and I_{Ks} can be identified by their gating kinetics and difference in sensitivity to drugs. In 1976, Noma and Irisawa described the presence of these currents in rabbit SA node cells (Noma & Irisawa, 1976).

I_K currents are responsible for repolarization, but the role of the different I_K components in the SA node varies between species. I_{Kr} seems to play an important role in rabbits, while, in guinea pig, I_K is mainly composed of I_{Ks} (Matsuura et al., 2002); in pig, I_{Kr} appears to be absent altogether (Ono et al., 2000). Functional data about I_K in human SA node are lacking, but mRNA for all three channels has been found in human SA node (Chandler et al., 2009).

2.4.1 Ultra-rapid component of the delayed rectifier K^+ current (I_{Kur})

Of the different components of I_K, least is known about the presence, function and role of the ultra-rapid component (I_{Kur}) in SA node. In 2000, Dobrzynski et al. proved the presence of Kv1.5, the α-subunit of the channel encoded by *KCNA5*, in guinea pig SA node by Western blotting and immunolabeling (Dobrzynski et al., 2000). As discussed previously, mRNA for Kv1.5 is present in human SA node.

This rapidly activating and non-deactivating current was first described in 1991 (Boyle & Nerbonne, 1991) and has since then been referred to as I_{ss} (steady-state), I_{sus} (sustained), and I_{Kur} (ultra-rapid) (Nerbonne, 2000). I_{Kur} activates around –40 mV and is blocked effectively with low concentrations of 4-AP (Boyle & Nerbonne, 1991). In 2003, the current was described in SA node of healthy and heart failure rabbits (Verkerk et al., 2003). Block of I_{Kur} with low concentrations of 4-AP (too low to block I_{to}) prolonged murine SA node cycle length by 20% (from 272±25 to 328±31 ms) (Nikmaram et al., 2008).

2.4.2 Rapid component of the delayed rectifier K^+ current (I_{Kr})

The α-subunit of I_{Kr} is encoded by Kv11.1 (also known as *hERG* or *KCNH2*). Mutations in this gene are found in patients with long QT syndrome type 2 (Curran et al., 1995). While expression of *hERG* in Xenopus oocytes confirmed the hypothesis that this gene encodes the α-subunit of I_{Kr}, differences between the expressed current and native current still existed (Sanguinetti et al., 1995). The role of the proposed β-subunit MiRP1 (minK related peptide 1, *KCNE2* gene) remains controversial (Abbott et al., 1999).

I_{Kr} shows inward rectification, meaning that the channel passes current more easily in the inward direction than the outward direction. This rectification is caused by very rapid inactivation that develops after activation of the channel by depolarization. Thus, very little I_{Kr} exists during the plateau phase of the action potential. During repolarization, there is recovery from inactivation causing an outward current responsible for late repolarization, followed by slow deactivation (Ono & Ito, 1995).

In rabbit SA node cells, I_{Kr} activation starts around –50 mV with a voltage of half maximal activation of -17.4 mV (Lei & Brown, 1996). Adrenergic stimulation of I_{Kr} has a dual effect. On the one hand, phosphorylation by PKA causes a reduction in current amplitude, faster deactivation and a depolarizing shift in voltage-dependence of activation. On the other hand, direct binding of cAMP to Kv11.1 causes a hyperpolarizing shift in voltage-dependence of activation. Whether this results in an increase or decrease of net current

depends on the presence of accessory proteins. In the absence of MiRP1, there is a decrease in current, while there is an increase in the presence of MiRP1 (Cui et al., 2000).
As mentioned above, the role of I_{Kr} differs between species. *ERG1B* knock out mice did not display a reduction in overall heart rate, but 6 out 21 mice did show abrupt and spontaneous bradycardias that were never seen in control littermates (Lees-Miller et al., 2003). In rabbit and mouse SA node cells, blockade of I_{Kr} with E-4031 prolonged cycle length and action potential duration, and depolarized the MDP (Clark et al., 2004; Verheijck et al., 1995). Since I_{Kr} is absent from pig SA node, blocking of I_{Kr} did not have any affect on the action potential or cycle length in this species (Ono et al., 2000).

2.4.3 Slow component of the delayed rectifier K^+ current (I_{Ks})

Until 1996, there was controversy about the proteins responsible for generating I_{Ks}. In 1988, the gene *IsK*, also known as minK (*KCNE1*), was cloned into Xenopus oocytes, resulting in a K^+ current resembling I_{Ks} (Takumi et al., 1988). Expression in other cell lines, however, did not result in the generation of a similar current, leading to the hypothesis that minK coassembles with other proteins present in Xenopus oocytes to form I_{Ks}. When a new K^+ channel was identified through positional cloning (Kv7.1), this channel was found to produce a current resembling I_{Ks} when co-expressed with its β-subunit, minK protein (Barhanin et al., 1996; Sanguinetti et al., 1996).
The α-subunit Kv7.1, encoded by *KCNQ1*, is formed by tetramerization of four 6-transmembrane segments (Nerbonne & Kass, 2005). Together with 2 minK proteins and the protein Yotiao, this tetramer forms a macromolecular complex (Lin et al., 1998). Apart from regulating current kinetics, interaction between Kv7.1 and minK within the endoplasmic reticulum stabilizes newly synthesized channels (Peroz et al., 2009).
In guinea pig ventricular myocytes, I_{Ks} activates slowly upon depolarization to potentials positive to –30 mV, with a voltage of half maximal activation around 26 mV (Balser et al., 1990). In rabbit SA node cells, a voltage of half maximal activation of 15.6 mV was found (Lei & Brown, 1996).
In 1991, Sanguinetti et al. reported experiments in which they showed that isoproterenol increases I_{Ks} in guinea pig ventricular myocytes (Sanguinetti et al., 1991). This responsiveness to β-adrenergic stimulation requires the presence of the β-subunit, minK protein, and Yotiao (Kurokawa et al., 2003; Marx et al., 2002), and involves phosphorylation of Kv7.1 by protein kinase A (Walsh & Kass, 1988). The increase in I_{Ks} upon β-adrenergic stimulation also augments its role in spontaneous activity: while blocking I_{Ks} in rabbit SA node cells has negligible effects on cycle length or MDP in control conditions, blockade during stimulation with isoproterenol led to an increase in cycle length, a depolarized MDP and slower diastolic depolarization (Lei et al., 2002). An increase in I_{Ks} due to β-adrenergic stimulation is also partly due to an increase in heart rate, since there is incomplete deactivation at high rates (Jurkiewicz & Sanguinetti, 1993).
The role of I_{Ks} in SA node function in human can only be deduced from patients with long QT syndrome type 1 (mutations in *KCNQ1*). Not only do these patients exhibit prolonged QT intervals, causing arrhythmias during exercise due to prolonged repolarization in ventricular tissue, they also have a diminished increase in heart rate upon exercise (Haapalahti et al., 2006). No I_{Ks} has been found in mouse SA node (Cho et al., 2003), and, as expected, *KCNQ1* knock out mice do not show prolongation of cycle length (Knollmann et al., 2004). Since I_{Ks} is the only I_K present in pig, spontaneous activity ceased on blocking I_{Ks} with chromanol 293B (Ono et al., 2000).

2.5 Inward rectifier K^+ current current (I_{K1})

The α-subunit of the inward rectifier K^+ current current (I_{K1}) is formed by tetramerization of four 2-membrane spanning domains that do not include a voltage sensor (Hibino et al., 2010). The α-subunit can be formed by homomerization or heteromerization of members of the Kir2.x subfamily. Kir2.1, the major component of the cardiac α-subunit of I_{K1}, is encoded by *KCNJ2* (Plaster et al., 2001).

I_{K1} is an inward rectifier which is blocked at potentials more positive than the equilibrium for K^+ (E_K), which lies at around –85 mV, by Mg^{2+} and polyamines (Lopatin et al., 1994; Matsuda et al., 1987). Figure 4A, left panel, shows a typical examples in an isolated rabbit left ventricular myocyte; the arrow indicates E_K. Due to the inward rectifying properties, I_{K1} is reduced during depolarization (Fig. 4B); this allows the action potential plateau phase to exists. During repolarization, the current is unblocked (Fig. 4B) and I_{K1} further repolarizes the membrane towards E_K. Importantly, negative and positive to E_K, I_{K1} is an inward and outward current, respectively. Consequently, I_{K1} will stabilize the membrane potential around E_K.

This current, which at first glance appears to antagonize spontaneous activity, is not present in rabbit SA node (Irisawa et al., 1993), and is negligibly small in murine and rat SA node cells (Cho et al., 2003; Shinagawa et al., 2000). Figure 4A, right panel, shows typical current traces in a rabbit SA node cell measured with a similar voltage clamp protocol and solutions as in the ventricular myocyte (left panel). Note the absence of I_{K1} in the SA node cell (arrow), which is also summarized in the I-V relationships in Figure 4B. Due to the fact that I_{K1} is absent or functionally negligibly small, SA node cells have a relatively positive MDP, at around –60 mV (Mangoni & Nargeot, 2008)

Knock-out of Kir2.1 in mouse resulted in no detectable I_{K1}, longer action potentials, and spontaneous activity in 70% of isolated ventricular cells. Knock-out of Kir2.2 resulted in a 50% reduction of I_{K1} without other abnormalities (Zaritsky et al., 2001). Since these mice died at young age due to cleft palate, mice expressing a dominant-negative construct were designed. These mice, who did not show facial abnormalities, showed a 90% reduction in I_{K1}. This was associated with a decrease in heart rate of 31% (McLerie & Lopatin, 2003). Whether this is a consequence of the reduction in I_{K1} in SA node cells or results from reduced electrical load imposed by the atrium remains to be resolved.

In 2009, Chan et al. proposed that I_{K1} may act to increase heart rates by enhancing I_f through its effect to maintain membrane potentials within a range where HCN channels can most effectively operate. By overexpressing *HCN1* and *KCNJ2,* both independently and together, in quiescent guinea pig ventricular myocytes, they showed that I_{K1} further increased automaticity that was already induced by *HCN1* overexpression (Chan et al., 2009). Not only was there an increase in beating rate (320 bpm vs 181 bpm), but there was also a more hyperpolarized MDP and an increase in I_f.

2.6 Voltage dependent Na^+ current (I_{Na})

The α-subunits of the voltage dependent Na^+ channels contains four homologous domains, all containing six transmembrane segments. Of the different α-subunits, several have been found to be present in murine SA node, including neuronal isoforms (Lei et al., 2004; Maier et al., 2003). In human SA node, Nav1.5 (*SCN5A*) mRNA was detected, although at lower levels than in paranodal and right atrial tissue. Nav1.2 (*SCN2A*) and Nav1.4 (S*CN4A*) mRNA was also identified in the SA node, but at negligible levels (Chandler et al., 2009).

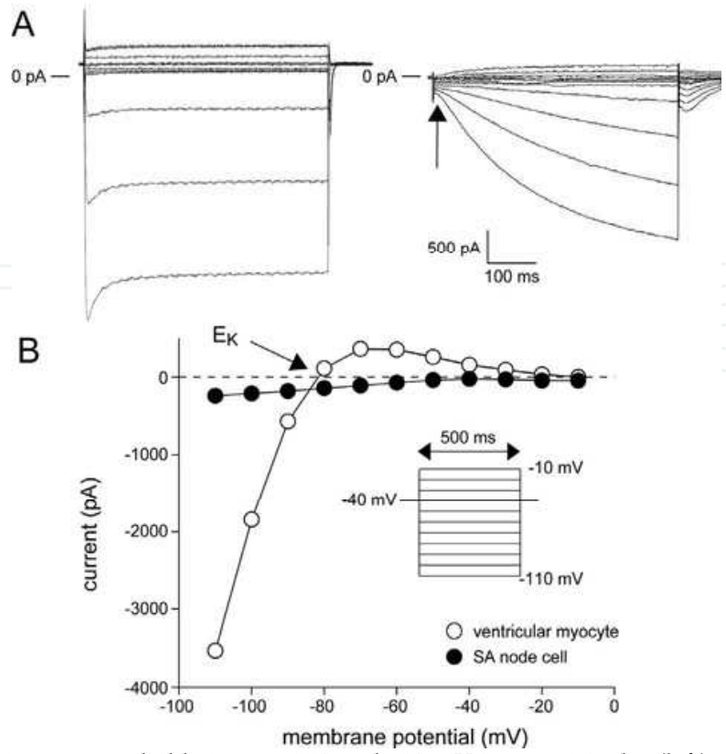

A, Typical current traces recorded between –110 and –10 mV in a ventricular (left) and SA node (right) cell of rabbit. Please note the absence of a prominent I_{K1} in the SA node cell (arrow). B, I-V relationships of the current measured in the beginning of the voltage clamp steps. The arrow indicates the reversal of current (E_K) in the ventricular myocyte. Inset, Voltage clamp protocol used.

Fig. 4. Inward rectifier K^+ current (I_{K1}) in ventricular and SA node cells.

However, in canine SA node, mRNA for Nav1.1 (*SCN1A*), 1.2, 1.3 (*SCN3A*), and 1.5 is present (Haufe et al., 2005). Expression of only α-subunits leads to functional Na^+ current (I_{Na}), but co-expression of β-subunits influences gating kinetics and current amplitude. So far, 4 different β-subunits (*SCN1B* to *SCN4B*) have been identified (Isom et al., 1995; Isom et al., 1992; Morgan et al., 2000; Yu et al., 2003).

Cardiac Na^+ channels open upon depolarizaton, allowing an influx of Na^+ ions, responsible for the rapid upstroke of the atrial and ventricular action potential. In 1975, Kreitner reported experiments in rabbit SA node preparations. She showed that tetrodotoxin (TTX), a blocker of I_{Na}, only negligibly affected spontaneous rate and action potential waveform. Carbamylcholine, a cholinergic agonist, hyperpolarized the MDP and increased the rate of rise of the action potential, suggesting a role for I_{Na} at more negative membrane potentials. Indeed, adding TTX after addition of carbamylcholine caused a decrease in the slope of depolarization. It was concluded that I_{Na} is present in the SA, but is inactivated under normal conditions, due to the relatively depolarized membrane potential of SA node cells (Kreitner, 1975). More recent studies, however, indicate a role for Na^+ channels in SA node pacemaking in newborn rabbit (Baruscotti et al., 2000).

In 2004, Lei et al investigated the role of the different α-subunits in adult mouse SA node cells. They showed that the I_{Na} present in these cells consisted of two components: one that is blocked by nanomolar concentrations of TTX and one that is blocked by micromolar concentrations. The neuronal isoforms are known to be more sensitive to block by TTX. In

intact preparations, both high and low concentrations caused an increase in cycle length, while only at high concentrations activity in the periphery ceased. Immunostaining showed the neuronal isoform Nav1.1 to be present in small and large cells throughout the SA node. Nav1.5, on the other hand, was not present in the center of the SA node. In 2010, Protas et al. showed that I_{Na} is present in 80% of canine SA node cells, with greater current densities at younger age. Due to inactivation at relatively negative potentials this current would be unavailable at physiological potentials, but might be recruited in case of hyperpolarization (Protas et al., 2010). Verkerk et al. had the opportunity to study ion currents in human SA node cells and showed that, upon switching off a hyperpolarizing pulse, there was a large inward current that rapidly activated and inactivated, probably I_{Na} (Verkerk et al., 2009b).
The notion that there is a role for I_{Na} in human SA node is further supported by the fact that mutations in *SCN5A* are known to influence sinus rate. Loss of function mutations in S*CN5A* have been associated with sick sinus syndrome (Benson et al., 2003).
Moreover, there is an overlap in I_{Na} activation and inactivation curves resulting in a window Na^+ current. It is suggested that such a Na^+ window current can be present at potentials found in SA node (Attwell et al., 1979; Muramatsu et al., 1996). Accordingly, late or persistent Na^+ current ($I_{Na,L}$), due to mutations in the *SCN5A* gene (Tan et al., 2003) may affect SA node function significantly. $I_{Na,L}$ due to mutation in SCN5A or drug use, induced SA node pacemaker slowing due to action potential prolongation and depolarization of the MDP (Veldkamp et al., 2003; Wu et al., 2008)
While homozygous *SCN5A* knock-out is embryonically lethal (Papadatos et al., 2002), heterozygous deletion of *SCN5A* in mouse results in lower heart rate and sino-atrial block (Lei et al., 2005)

2.7 Sustained inward current (I_{st})

Relatively little is known about the sustained inward current (I_{st}), a current first described in rabbit SA node in 1995 (Guo et al., 1995). So far, the molecular structure of the channels is unknown. I_{st} is an inward current that is activated upon depolarization to –60 mV and that shows pharmacological characteristics resembling those of the voltage-gated Ca^{2+} channels, including sensitivity to nicardipine and resistance to TTX, but is carried by Na^+ (Guo et al., 1995). The first single channel measurements followed a few years later, showing the current to be absent from quiescent cells, to activate at potentials positive to -80mV, and to reverse at 13 mV (Mitsuiye et al., 2000).
β-Adrenergic stimulation shifts the threshold for activation and the potential of maximum amplitude to more negative potentials (Cho et al., 2003; Huang et al., 2008; Toyoda et al., 2005). Acetylcholine (ACh) does not have an inhibitory effect in an unstimulated situation, but, after stimulation with isoproterenol, ACh causes a reduction in amplitude (Toyoda et al., 2005).
The role in spontaneous activity is difficult to assess, considering the overlap with $I_{Ca,L}$ in drug sensitiviy. Taurine, which increases I_f and $I_{Ca,T}$ but decreases I_{st} and $I_{Ca,L}$, inhibits spontaneous activity in rat SA node cells, implying that the decrease in I_{st} and $I_{Ca,L}$ is more important than increase in I_f and $I_{Ca,T}$ in controlling beating rate (Satoh, 2003).
Action potential clamp studies show I_{st} to be present in control conditions over the entire voltage rage of guinea pig SA node cells, with a maximum around –20 mV. Since this inward current is present within the voltage range of the diastolic depolarization, part of the depolarization seems to be caused by I_{st}. In silico models of SA cells consistently show an

increase in beating rate upon incorporation of I_{st}, varying from an increase of 0.8% to 20% (Zhang et al., 2002a).

2.8 Other currents

2.8.1 Background current (I_{Ba})

The equilibrium for K^+ lies around -85mV and the SA node MDP is less negative, suggesting a greater conductance for Na^+ than K^+. In the absence of $I_{K1,}$ there is indeed a low permeability for K^+. In 1995, a background current carried by Na^+ (I_{Ba}) was shown in rabbit SA. After inhibition of K^+ currents, I_f, I_{NCX}, Ca^{2+} currents and the Na^+/K^+ pump, this background current was inward at potentials negative to -21 mV (Hagiwara et al., 1992).

2.8.2 Na^+-K^+ pump current (I_p)

This current, generated by the electrogenic Na^+/K^+ pump (I_p), is responsible for keeping intracellular Na^+ concentration low and the K^+ concentration high by extruding 3 Na^+ from the cell in exchange for 2 K^+. In a solution containing 5 mM K^+, rabbit SA node strips had an MDP of -58 mV. Upon exchanging this fluid for a K^+-free solution, there was depolarization with initially an increase in beating rate, eventually resulting in oscillation. When again K^+ was added again to a concentration of 5 mM, hyperpolarization occurred and spontaneous activity resumed. Ouabain, a Na^+/K^+ pump blocker, or replacement of Na^+ with Li^+, prevented this hyperpolarization, suggesting a role for I_p (Noma & Irisawa, 1975; Noma & Irisawa, 1974). With a voltage of half maximal activation of -52 mV and a current magnitude of 22.5 pA, this outward current could partly control normal pacemaking by counterbalancing inward currents (Sakai et al., 1996).

2.8.3 ACh-activated K^+ current ($I_{K,ACh}$)

The K^+ current activated by ACh ($I_{K,ACh}$) is involved in the negative chronotropic effect of ACh by hyperpolarizing the cell (Noma & Trautwein, 1978). The proteins responsible for the tetramers, Kir3.1 (KCNJ3) and Kir3.4 (*KCNJ5*), were indeed identified by immunofluorescence in rat SA node (Dobrzynski et al., 2001). Apart from the direct and short lasting hyperpolarizing effect of $I_{K,ACh}$ on the SA node, the increase in $I_{K,ACh}$ in surrounding atrial muscle leads to a longer lasting effect on the SA node by electrotonic interaction (Kodama et al., 1996).

2.8.4 ATP-sensitive current ($I_{K,ATP}$)

Activation of ATP sensitive current $I_{K,ATP}$ by depletion of ATP or by $I_{K,ATP}$ openers (pinacidil, cromakalim, nicorandil) hyperpolarizes the diastolic membrane potential by activation of an outward K^+ current with a reversal potential around E_K which is sensitive to the $I_{K,ATP}$ blocker glibenclamide (Han et al., 1996; Satoh, 2003). Knock out of Kir6.2 (*KCNJ11*), the α-subunit of $I_{K,ATP}$ channels, results in a diminished response to hypoxia both in Langendorff perfused hearts and in isolated SA node cells. The decrease in beating rate seen in wild type mice can presumably prevent against ischemia induced damage (Fukuzaki et al., 2008).

3. Anatomy of the SA node

3.1 Location of the SA node

After the location of the SA node was first described in 1907 (Keith & Flack, 1907), the anatomy of this structure has been found to vary among species. While the node is always

identified at the junction of the right atrium and superior caval vein, there is considerable variation. In human, dog, and pig the SA node lies epicardially, while in rabbit it covers the entire thickness of the intercaval region and part of the endocardial surface of the crista terminalis (Boyett et al., 2000; Opthof, 1988). Additionally, while man, monkey, dog, pig, and horse have a central SA node artery, there is none in rabbit, guinea pig, and cat (Opthof, 1988). In man, the SA node artery originates from the right coronary artery in 55% of cases, and from the circumflex branch of the left coronary artery in the remainder. In rat, blood supply comes from the internal mammary artery, which is a very relevant aspect to take into account when studying Langendorff perfused hearts (James, 2002).

3.2 Different cells within the SA node

The SA node exhibits changes in electrophysiological characteristics from center to periphery. The cause of this heterogeneity has led to some debate (for review see Boyett et al., 2000). Whether there is a gradual change in cell type from SA node center to atrium (gradient model) or a change in composition of cells (mosaic model), still remains to be resolved. The mosaic model states that there are no differences between single cells isolated from the center or periphery of the SA node, but that the differences found in intact preparations are based on the differences in the amount of atrial cells within the tissue, with 41% of cells in the center, and 63% of cells in the periphery being atrial atrial cells. Supporting this hypothesis are the findings that not all myocytes within the SA node stain with neurofilament antibody (used to characterize SA node cells), and that cell isolation within the intercaval region results in typical SA node cells and atrial cells (Verheijck et al., 1998). In their response to this article, Zhang et al. consider a few arguments ontradicting this theory (Zhang et al., 2001a). Firstly, they use data from three different studies showing that, when the SA node and surrounding atrial tissue are intact, the leading pacemaker site is the center of the SA node, while, when different parts are separated, the more peripheral regions show faster spontaneous activity. This argument, however, does not account for the fact that, according to the mosaic model, these parts contain more atrial cells, and the hyperpolarizing effect of these cells might increase beating rate, just like overexpression of I_{K1} can increase beating rate (Chan et al., 2009). Under normal conditions, the extra load of the attached atrial muscle might prevent a more peripheral start of activation by electrotonic influence. However, when the mosaic model was tested in silico, by making two square lattices of 20x20 cells filled with nodal cells and either 41 or 63% atrial cells with a coupling conductance between cells of 0 to 25 nS, a faster intrinsic rate was found in the more central (41% atrial cells) than peripheral (63% atrial cells) lattice (Zhang et al., 2001a). Other data supporting the gradient cell model are the differences in electrophysiological characteristics found in small and large cells, originating from the center and periphery of the SA node, respectively. Action potential amplitude, MDP, take-off potential, action potential upstroke velocity, rate of diastolic depolarization, and spontaneous beating rate are faster in larger cells, combined with a larger density in I_f and I_{Na} (Honjo et al., 1996).

Within the SA node, there is a remarkable amount of connective tissue: islands of nodal cells are separated by connective tissue (De Maziere et al., 1992). While, at first, myocytes were thought to be electrically isolated from non-excitable cells, immunohistochemical labelling has shown that fibroblasts surrounded by other fibroblasts express connexin40, while fibroblasts adjacent to nodal cells express connexin45. Moreover, functional testing showed occasional spread of Lucifer yellow between adjacent myocytes and fibroblasts (Camelliti et

al., 2004). The functional role of the connections between nodal cells and fibroblasts needs further studying, but, theoretically, fibroblasts could have different functions in the SA node. To begin with, they can function as a current sink, possibly affecting spontaneous activity. Secondly, because cardiac fibroblasts are thought to be mechanosensitive, they are thought to play a role in the positive chronotropic response to stretch of the right atrium (Kohl et al., 1994). Finally, although not being electrically active themselves, fibroblasts can conduct an electrical signal between myocytes (Kohl et al., 2005).

3.3 Coupling within the SA node and between SA node and right atrium

Despite the fact that the SA node is relatively small and the atrium is more hyperpolarized, the SA node is capable of generating impulses and propagating these to the surrounding tissue. The question how the SA node is capable of doing this was first studied using in vitro models. It was shown that a low coupling resistance between SA node and atrium would inhibit impulse generation by electrotonic interaction. On the other hand, if coupling resistance becomes too high, the SA node will be able to generate impulses, but these impulses will not be propagated to the atrium. Optimal pacemaking and conduction was reached with a low conductance within the SA node and a gradual increase of coupling towards the periphery (Joyner & van Capelle, 1986). Interdigitation of atrial strand within the SA node was found by immunolabeling (Oosthoek et al., 1993; ten Velde et al., 1995). This interdigitation was shown to have beneficial effects on impulse conduction from SA node to atrium (Winslow & Varghese, 1995). The intermingling of strands of atrial tissue within the SA node prevents the SA node from too strong a hyperpolarizing influence, while the atrial strands can propagate the action potential.

The electrotonic effect of the atrium can also protect the SA node. Blocking I_{Kr} results in a depolarization of the SA node, without affecting atrial resting membrane potential. This never results in pacemaker arrest. When the atrium is removed, blocking I_{Kr} results in pacemaker arrest, showing a beneficial effect of the electrotonic influence of the atrium (Verheijck et al., 2002).

The question is how well SA node cells are coupled to each other and to atrial cells. First of all, very little coupling is necessary between two SA node cells for entrainment (Verheijck et al., 1998; Wilders et al., 1996). Since two rabbit SA node cells with a 26% difference in interbeat interval require a coupling conductance of only 0.17 nS for frequency entrainment, and conductance of sinatrial node gap junctional channels can be ~75 pS, only 3 gap junctional channels would suffice (Verheijck et al., 1998). The slow conduction velocity within the SA node and the low space constant are signs of the limited electrical coupling between the cells (Boyett et al., 2000).

Gap junction channels allow for intercellular cytoplasmic communication. Connexins (Cx) form hemichannels called connexons. In the heart, several different connexins are found, including Cx43 in working myocardium, and Cx40 and Cx45 in conduction system. These different connexins can generate a variety of gap junctions with different properties, including conductance (Veenstra et al., 1992). Studies on the different connexins present in SA node are contradictory, but most studies have not shown Cx43 in rabbit SA node, and have found Cx40 and Cx45. These studies are complicated by the difficulty in finding subtype specific antibodies and the scarcity of the amount of connexins within the SA node. In human SA node, mRNA of Cx40, Cx43, Cx45 and negligible amounts of Cx31.9 were identified (Chandler et al., 2009).

4. Autonomic modulation of the SA node

Almost all of the ionic currents discussed so far are sensitive to autonomic modulation. However, the response of the SA node to different stimuli cannot be easily predicted due to the heterogeneity of, and interaction between, the cells. Basic heart rate results from a balance between sympathetic and parasympathetic input, which may differ between species. In rabbit, like in rodents, sympathetic tonus dominates, since the beating rate of isolated right atrium is much lower than in vivo rate. In dog and human, parasympathetic tonus prevails (Opthof, 2000). When studying (para-) sympathetic stimulation, it is always relevant to realize that addition of a substance, for example adrenalin, might give a very different response than nerve stimulation (Choate et al., 1993).

4.1 Sympathetic stimulation

Activation of the β-adrenergic receptor (β-AR) by catecholamines can give rise to a multitude of changes. Activation of the β-ARs, a G-protein coupled receptor, leads to stimulation of the stimulatory G-protein (G_s), whereby adenylyl cyclases are activated and cAMP is formed. CAMP can either bind directly to ion channels or influence their function by activating protein kinase A (PKA). PKA can in turn, by phosphorylation, influence the function of other proteins, including ion channels,.

Both β1- and β2-adrenergic receptors are present in SA node (Hedberg et al., 1980), differing in their coupling to G-proteins en localization within the cell membrane. While β1-ARs are coupled to only stimulatory G-proteins, β2-ARs are coupled to both stimulatory and inhibitory G-proteins (Xiao et al., 1999). This can account for the shorter duration of the positive chronotropic effect of β2-adrenergic stimulation compared to stimulation of the β1-AR (Devic et al., 2001). Furthermore β2-adrenergic receptors have been found to localize to caveolae, specific regions of the cell membrane, while β1-ARs do not (Barbuti et al., 2004).

The changes induced by β-adrenergic stimulation include an increase in I_f, $I_{Ca,L}$, I_{Kr}, I_{Ks}, and I_{st}, and an increase in spontaneous Ca^{2+} releases from the sarcoplasmic reticulum, all supporting either faster diastolic depolarization or a shorter action potential duration, causing an increase in beating rate.

The response to β-adrenergic stimulation is not equal among different areas of the SA node, causing a shift in site of earliest activation upon stimulation (Mackaay et al., 1980).

4.2 Parasympathetic stimulation

Parasympathetic modulation not only involves modulation of the currents usually active by decreasing the cAMP concentration, but as mentioned previously also involves activation of $I_{K,ACh}$ (Noma & Trautwein, 1978).

After stimulation of the M2-receptor, different phases in heart rate response can be detected: first there is a decrease in rate, followed by a short increase, and afterwards again a decrease. The first decrease is thought to be the result of a direct effect of ACh on SA node, the second decrease a result of the hyperpolarizing effect of the atrium upon the SA node. The effect of ACh is exaggerated in the presence of noradrenalin (Levy, 1971).

As with sympathetic stimulation, the response to parasympathetic stimulation is also not homogeneous within the SA node. While the primary pacemaker is very sensitive and will increase cycle length considerably, other parts that have a lower intrinsic frequency are less sensitive and will take over as the site of earliest activation (Mackaay et al., 1980). This heterogeneity prevents too slow bradycardia or asystole from occurring.

5. Creation of a biopacemaker

When working on the creation of a biopacemaker, several issues need be kept in mind. To begin with, the goal should not be the recreation of an SA node. Apart from the simple fact that a complicated structure like the SA node can not easily be reconstructed, this might not be necessary. The biopacemaker is not required to generate a rhythm in the same way the SA node does, as long as it generates a stable rhythm. For instance, while the biopacemaker is a therapy to be used in clinical situations where the heart is no longer paced sufficiently by the SA node, it does not need to be capable of generating a heart rhythm during the development of the heart. Secondly, longevity is required. This is especially relevant when choosing a delivery strategy, as will be discussed in paragraph 5.2. Also, the biopacemaker should be responsive to autonomic modulation, as is the SA node. Finally, and most importantly, safety should be a priority when considering gene or cell therapy.

5.1 How to generate rhythm

As is clear from the previous paragraphs, the SA node cells contains multiple ion channels that can facilitate the generation of spontaneous activity. However, not only SA node cells contain these ion channels. Although the rate of automatic activity might be slower, spontaneous activity is also present in cells from the atrium, atrioventricular (AV) node, and Purkinje fibers. And even though ventricular cells might not be active, the machinery to generate spontaneous activity is present, albeit repressed by a high activity of I_{K1}.

The first study published on biopacemaking used the spontaneous activity already present. By injection of a plasmid carrying human β2-adrenergic receptor cDNA into the right atrium of mice, heart rate temporarily increased (Edelberg et al., 1998). Others have used the intrinsic capacity of ventricular cells to generate rhythm by increasing the level of cAMP in the cell by temporary overexpression of adenylyl cyclase VI (Ruhparwar et al., 2010). After injection of adenovirus containing the AC-VI gene in the left ventricle of pig, and after ablation of the AV node, all animals showed an escape rhythm coming from the left ventricle after rapid ventricular pacing and administration of isoprenalin, while, in control animals, right ventricular escape rhythms were observed. Maybe the most elegant way of using the cells' own ability to generate a rhythm so far has been to inhibit the cells own suppression on spontaneous activity, i.e., I_{K1}. Overexpression of a Kir2.1 dominant negative construct led to a 80% reduction in I_{K1} and spontaneous beating in cells originating from the left ventricle (Miake et al., 2002).

Another way to generate spontaneous activity is the introduction of depolarizing currents into normally quiescent cells. The most obvious target is I_f, as this current activates at potentials negative to -50 mV and this means the current is active at normal atrial and ventricular resting membrane potentials (Verkerk et al., 2007b).

This started when in 2001 Qu et al. overexpressed murine *HCN2* in spontaneously beating neonatal ventricular myocyte cell cultures, leading to a more regular and faster rhythm, due to diastolic phase 4 depolarization (Qu et al., 2001). In 2003, they described experiments in which they used this adenoviral construct in order to overexpress *HCN2* in the left atrial appendage in dog. Several days after subepicardial injection of the construct, dogs underwent vagal stimulation in order to suppress sinus rhythm. During vagal stimulation, all dogs injected with Ad-*mHCN2* showed spontaneous activity originating from the atrium, which was not seen in control dogs (Ad-GFP) (Qu et al., 2003). The introduction of a mutant *HCN2* channel in left ventricle by Bucchi et al. in dogs with permanent AV-block showed a

modest advantage of the mutant channel regarding response to catecholamines (Bucchi et al., 2006).

Since *HCN4* is the predominant isoform of I_f in the SA node, Boink et al. overexpressed this gene in rat cardiac myocytes using a lentiviral vector (Boink et al., 2008). In cell cultures, this led to an increase in beating rate, responsive to autonomic stimulation by cAMP.

A novel approach was used by Xiao et al who interfered in the microRNA pathway in order to overexpress *HCN2* and *HCN4* in vitro (Xiao & Sigg, 2007). MicroRNAs are small non-coding RNAs that bind to mRNA, thereby decreasing translation. *HCN2* and *HCN4* translation are regulated by miR-1 and miR-133. By masking the microRNA binding sites with gene specific oligodeoxynucleotides on *HCN2*/*HCN4* mRNA, protein expression of *HCN2* increased by 70% and *HCN4* by 45% in cultured ventricular myocytes, causing an increase in beating rate of monolayer culture.

As previously discussed, the synergistic effect of overexpression of I_{K1} and I_f leads to an increased beating rate in isolated guinea-pig ventricular cells compared to only overexpression of I_f, due to maintenance by I_{K1} of the voltage range wherein I_f can function optimally (Chan et al., 2009).

Other currents that can be considered are $I_{Ca,T}$, $I_{Ca,L}$, I_{NCX}, and I_{st}. Regarding $I_{Ca,T}$: as mentioned above, the different isoforms of $I_{Ca,T}$ show different activation kinetics, with Cav3.3 activating at potentials positive to -80 mV (McRory et al., 2001). This might make it useful in cells with a relatively depolarized resting membrane potential, but in ventricular cells with a stable resting membrane potential around -85 mV, the contribution might be negligible. The same is true for $I_{Ca,L}$, which activates at potential positive to -60 mV (Verheijck et al., 1999), but the advantage of this current is its sensitivity to β-adrenergic stimulation. Since the theory of the 'Ca^{2+} clock' states that spontaneous activity depends on spontaneous Ca^{2+} releases from the sarcoplasmic reticulum (Maltsev et al., 2006), it could be possible that overexpression of proteins involved in either sarcoplasmic Ca^{2+} loading (e.g., sarco/endoplasmic reticulum Ca^{2+}-ATPase - SERCA) or Ca^{2+} release (the Ryanodine receptor - RyR) increase spontaneous activity. *NCX1* transgene mice showed a 2,5-fold higher protein level of *NCX1* expression without alterations in SERCA, the Na^+/K^+ pump, phospholamban, and ryanodine receptor. This led to a 42% increase in *NCX1* current amplitude and a higher SR Ca^{2+} content, but no change in heart rate (Wang et al., 2009). A similar study using overexpression of *SERCA2A* also did not show an effect on basic heart rate or heart rate after isoproterenol (He et al., 1997). However, these studies were done in animals with normal SA node function. When it comes to I_{st}, there might be another problem. I_{st} seems to be a good candidate when it comes to activation kinetics. However, since the molecular background remains to be clarified, it is currently not a reasonable option.

While it might seem easiest to use one of the ion channels already present in SA node, it is, of course, also possible to modify existing proteins to generate a current suitable for biopacemaking. This can be done by making small adjustments, like using a modified *HCN2* channel with faster activation kinetics (Plotnikov et al., 2008), but bigger adjustments are also possible. By changing both kinetics and ion selectivity, Kashiwakura et al. turned the human Kv1.4 depolarization-activated K^+ channel into a hyperpolarization-activated, nonselective channel (Kashiwakura et al., 2006). Gene transfer to ventricular myocytes indeed initiated spontaneous activity.

5.2 Gene therapy, cell therapy, or both?

Most studies discussed so far have used adenovirus as the vector transferring the cDNA into the host cells (for a review on the use of viral vectors in cardiac therapy see Gray & Samulski, 2008). While adenovirus has advantages, e.g., high titers, the capability to transduce both dividing and non-dividing cells, and the capability to transfer large cDNA molecules, there are also downsides. Most importantly, it cannot be used for long-term expression, since the cDNA is not incorporated into the host genome. This might not make it useful for long-term expression, but the fast transgene expression makes it very useful for short-term proof-of-principle studies. Apart from the lack of genome incorporation, high immunogenicity also poses a big problem, especially since it is a common pathogen. Other viral vectors that can be used are adeno-associated virus vectors and lentiviral vectors. Advantages of adeno-associated virus are the capacity to transduce dividing and non-dividing cells, cardiac tropism of certain subtypes, its mild immunogenicity and relatively long-lasting expression. A major restriction is the limited size of 4.6 kb (Grieger & Samulski, 2005). By their larger packaging size, lower immunogenicity, and their capability to integrate their genome into the host genome, lentiviruses seem to evade the limitations of the other types of viral vectors. The integration of viral DNA within the host genome at the same time forms the chief concern: that of carcinogenicity.

To circumvent these obstacles, Potapova et al. used genetically engineered human mesenchymal stem cells (hMSCs) transfected with murine *HCN2* to deliver pacemaker current (Potapova et al., 2004). Since hMSCs lack necessary ion channels, they are not capable of generating an action potential themselves. However, they are capable of spreading the depolarizing current to connected cardiomyocytes, which may cause an action potential in these coupled myocytes. As anticipated, co-cultures with canine ventricular myocytes and hMSCs overexpressing *HCN2* showed a higher spontaneous beating rate and a less negative MDP than control cultures with hMSCs overexpressing EGFP. When injected into canine heart, *HCN2* overexpressing hMSCs induced a faster ventricular escape rhythm, mapped to the site of cell injection, than seen in controls.

While the hMSCs are not spontaneously active, one could also use spontaneously active embryonic stem cells (Kehat et al., 2004) or fetal cardiomyocytes (Ruhparwar et al., 2002). By transplanting fetal atrial and SA nodal myocytes in the left ventricle of dogs that later underwent AV node ablation, a ventricular escape rhythm originating from the transplantation site was seen. Transplanted cells could later be identified by dystrophin immunoreactivity because they were coming from wildtype dogs, while host dogs did not express dystrophin. Expression of connexin 43 between donor and host cells suggests not only survival, but also electrical integration. However, with cell therapy, carcinogenicity remains a risk. Apart from that, the duration of the effect is not certain, one can imagine that stem cells which are coupled to adult myocytes differentiate and would lose their ability to generate spontaneous action potentials.

5.3 Location

The site of biopacemaker creation has varied between the different studies, including atrium, the ventricular conduction system, and a distinct region in the left ventricular free wall; also a more generalized approach with pacemaker creation throughout the left ventricle was published. Placement of a biopacemaker in the atria has an important limitation in that it depends on intact AV-node function. Advantages are intact atrio-ventricular synchronization, the fact that atrial cells already show spontaneous activity,

albeit at low frequency, and extensive innervation of the atria. This means only small modifications might be needed in order to generate a stably functioning biopacemaker sensitive to autonomic modulation. This advantage is shared by cells from the ventricular conduction system, while circumventing the disadvantage that normal AV node function is required. If the biopacemaker is placed relatively high in the conduction system, for instance the His bundle, this would also ensure a normal sequence of activation of the ventricles, maximizing cardiac output. So far, most studies have chosen injection of either cells or virus in the left ventricular free wall, probably because of the relatively easy access, especially relevant when using small animals.

5.4 Autonomic modulation

In the SA node, there is a heterogeneous response to sympathetic and parasympathetic stimulation. Due to this heterogeneous response, the SA node is capable of functioning within a wide range of heart rates. Since the cells with the lowest spontaneous rate are least sensitive to ACh, they serve as a back-up when the faster cells are made slower or even quiescent in the presence of ACh. The biopacemaker will most probably not be so heterogeneous, and for this reason it is of the utmost importance that it is not too sensitive to parasympathetic stimulation. As discussed in a review by Opthof, this makes I_f an appropriate target (Opthof, 2007), since it is mainly the opening of $I_{K,Ach}$ that decelerates rate and not a decrease in I_f during parasympathetic stimulation.

While sensitivity to parasympathetic stimulation should be limited, the great advantage of the biopacemaker should be its ability to increase rate upon physical or emotional stress.

6. Conclusion

As discussed in this chapter, the electrophysiology and anatomy or the SA node are complex. Therefore, it is not feasible to create a biopacemaker with all features of a native pacemaker. The most important issue for the creation of a biopacemaker is, that by adding an inward, or by reducing an outward current, working myocytes will be capable of stable action potential formation and propagation to the ventricles. While various approaches have been tried, so far a long-living biopacemaker suitable for clinical use, has not been developed. Further studies are required.

7. Reference

Abbott, G.W. et al. (1999). MiRP1 forms IKr potassium channels with HERG and is associated with cardiac arrhythmia. Cell, 97, 2, 175-187,

Accili, E.A. et al. (1997). Differential control of the hyperpolarization-activated current (i(f)) by cAMP gating and phosphatase inhibition in rabbit sino-atrial node myocytes. J. Physiol, 500 (Pt 3), 643-651,

Aimond, F. et al. (2005). Accessory Kvbeta1 subunits differentially modulate the functional expression of voltage-gated K+ channels in mouse ventricular myocytes. Circ. Res., 96, 4, 451-458,

Altomare, C. et al. (2003). Heteromeric HCN1-HCN4 channels: a comparison with native pacemaker channels from the rabbit sinoatrial node. J. Physiol, 549, Pt 2, 347-359,

Arechiga-Figueroa, I.A. et al. (2010). Multiple effects of 4-aminopyridine on feline and rabbit sinoatrial node myocytes and multicellular preparations. Pflugers Arch., 459, 3, 345-355,

Attwell, D. et al. (1979). The steady state TTX-sensitive ("window") sodium current in cardiac Purkinje fibres. Pflugers Arch., 379, 2, 137-142,

Balser, J.R. et al. (1990). Time-dependent outward current in guinea pig ventricular myocytes. Gating kinetics of the delayed rectifier. J. Gen. Physiol, 96, 4, 835-863,

Barbuti, A. et al. (2004). Localization of pacemaker channels in lipid rafts regulates channel kinetics. Circ. Res., 94, 10, 1325-1331,

Barhanin, J. et al. (1996). K(V)LQT1 and lsK (minK) proteins associate to form the I(Ks) cardiac potassium current. Nature, 384, 6604, 78-80,

Baruscotti, M. et al. (2005). Physiology and pharmacology of the cardiac pacemaker ("funny") current. Pharmacol. Ther., 107, 1, 59-79,

Baruscotti, M. et al. (2000). Na(+) current contribution to the diastolic depolarization in newborn rabbit SA node cells. Am. J. Physiol Heart Circ. Physiol, 279, 5, H2303-H2309,

Bean, B.P. (1985). Two kinds of calcium channels in canine atrial cells. Differences in kinetics, selectivity, and pharmacology. J. Gen. Physiol, 86, 1, 1-30,

Benitah, J.P. et al. (2010). L-type Ca(2+) current in ventricular cardiomyocytes. J. Mol. Cell Cardiol., 48, 1, 26-36,

Benson, D.W. et al. (2003). Congenital sick sinus syndrome caused by recessive mutations in the cardiac sodium channel gene (SCN5A). J. Clin. Invest, 112, 7, 1019-1028,

Bichet, D. et al. (2000). The I-II loop of the Ca2+ channel alpha1 subunit contains an endoplasmic reticulum retention signal antagonized by the beta subunit. Neuron, 25, 1, 177-190,

Blaustein, M.P. & Lederer, W.J. (1999). Sodium/calcium exchange: its physiological implications. Physiol Rev., 79, 3, 763-854,

Bohn, G. et al. (2000). Expression of T- and L-type calcium channel mRNA in murine sinoatrial node. FEBS Lett., 481, 1, 73-76,

Boink, G.J. et al. (2008). Engineering physiologically controlled pacemaker cells with lentiviral HCN4 gene transfer. J. Gene Med., 10, 5, 487-497,

Boyett, M.R. et al. (2000). The sinoatrial node, a heterogeneous pacemaker structure. Cardiovasc. Res., 47, 4, 658-687,

Boyle, W.A. & Nerbonne, J.M. (1991). A novel type of depolarization-activated K+ current in isolated adult rat atrial myocytes. Am. J. Physiol, 260, 4 Pt 2, H1236-H1247,

Brioschi, C. et al. (2009). Distribution of the pacemaker HCN4 channel mRNA and protein in the rabbit sinoatrial node. J. Mol. Cell Cardiol., 47, 2, 221-227,

Brown, H. et al. (1979). Cardiac pacemaker oscillation and its modulation by autonomic transmitters. J. Exp. Biol., 81, 175-204,

Bucchi, A. et al. (2006). Wild-type and mutant HCN channels in a tandem biological-electronic cardiac pacemaker. Circulation, 114, 10, 992-999,

Camelliti, P. et al. (2004). Fibroblast network in rabbit sinoatrial node: structural and functional identification of homogeneous and heterogeneous cell coupling. Circ. Res., 94, 6, 828-835,

Chan, Y.C. et al. (2009). Synergistic effects of inward rectifier (I) and pacemaker (I) currents on the induction of bioengineered cardiac automaticity. J. Cardiovasc. Electrophysiol., 20, 9, 1048-1054,

Chandler, N.J. et al. (2009). Molecular architecture of the human sinus node: insights into the function of the cardiac pacemaker. Circulation, 119, 12, 1562-1575,

Chen, C.C. et al. (2003). Abnormal coronary function in mice deficient in alpha1H T-type Ca2+ channels. Science, 302, 5649, 1416-1418,

Cho, H.S. et al. (2003). The electrophysiological properties of spontaneously beating pacemaker cells isolated from mouse sinoatrial node. J. Physiol, 550, Pt 1, 169-180,

Choate, J.K. et al. (1993). Effects of sympathetic nerve stimulation on the sino-atrial node of the guinea-pig. J. Physiol, 471, 707-727,

Clark, R.B. et al. (2004). A rapidly activating delayed rectifier K+ current regulates pacemaker activity in adult mouse sinoatrial node cells. Am. J. Physiol Heart Circ. Physiol, 286, 5, H1757-H1766,

Colecraft, H.M. et al. (2002). Novel functional properties of Ca(2+) channel beta subunits revealed by their expression in adult rat heart cells. J. Physiol, 541, Pt 2, 435-452,

Cui, J. et al. (2000). Cyclic AMP regulates the HERG K(+) channel by dual pathways. Curr. Biol., 10, 11, 671-674,

Curran, M.E. et al. (1995). A molecular basis for cardiac arrhythmia: HERG mutations cause long QT syndrome. Cell, 80, 5, 795-803,

De Jongh, K.S. et al. (1990). Subunits of purified calcium channels. Alpha 2 and delta are encoded by the same gene. J. Biol. Chem., 265, 25, 14738-14741,

De Maziere, A.M. et al. (1992). Spatial and functional relationship between myocytes and fibroblasts in the rabbit sinoatrial node. J. Mol. Cell Cardiol., 24, 6, 567-578,

Decher, N. et al. (2003). KCNE2 modulates current amplitudes and activation kinetics of HCN4: influence of KCNE family members on HCN4 currents. Pflugers Arch., 446, 6, 633-640,

Devic, E. et al. (2001). Beta-adrenergic receptor subtype-specific signaling in cardiac myocytes from beta(1) and beta(2) adrenoceptor knockout mice. Mol. Pharmacol., 60, 3, 577-583,

Dobrzynski, H. et al. (2007). New insights into pacemaker activity: promoting understanding of sick sinus syndrome. Circulation, 115, 14, 1921-1932,

Dobrzynski, H. et al. (2001). Distribution of the muscarinic K+ channel proteins Kir3.1 and Kir3.4 in the ventricle, atrium, and sinoatrial node of heart. J. Histochem. Cytochem., 49, 10, 1221-1234,

Dobrzynski, H. et al. (2000). Presence of the Kv1.5 K(+) channel in the sinoatrial node. J. Histochem. Cytochem., 48, 6, 769-780,

Edelberg, J.M. et al. (1998). Enhancement of murine cardiac chronotropy by the molecular transfer of the human beta2 adrenergic receptor cDNA. J. Clin. Invest, 101, 2, 337-343,

Foell, J.D. et al. (2004). Molecular heterogeneity of calcium channel beta-subunits in canine and human heart: evidence for differential subcellular localization. Physiol Genomics, 17, 2, 183-200,

Fukuzaki, K. et al. (2008). Role of sarcolemmal ATP-sensitive K+ channels in the regulation of sinoatrial node automaticity: an evaluation using Kir6.2-deficient mice. J. Physiol, 586, Pt 11, 2767-2778,

Gao, T. et al. (1997). Identification and subcellular localization of the subunits of L-type calcium channels and adenylyl cyclase in cardiac myocytes. J. Biol. Chem., 272, 31, 19401-19407,

Giles, W.R. & van Ginneken, A.C. (1985). A transient outward current in isolated cells from the crista terminalis of rabbit heart. J. Physiol, 368, 243-264,

Gray, S.J. & Samulski, R.J. (2008). Optimizing gene delivery vectors for the treatment of heart disease. Expert. Opin. Biol. Ther., 8, 7, 911-922,

Grieger, J.C. & Samulski, R.J. (2005). Packaging capacity of adeno-associated virus serotypes: impact of larger genomes on infectivity and postentry steps. J. Virol., 79, 15, 9933-9944,

Guo, J. et al. (1995). A sustained inward current activated at the diastolic potential range in rabbit sino-atrial node cells. J. Physiol, 483 (Pt 1), 1-13,

Haapalahti, P. et al. (2006). Ventricular repolarization and heart rate responses during cardiovascular autonomic function testing in LQT1 subtype of long QT syndrome. Pacing Clin. Electrophysiol., 29, 10, 1122-1129,

Haase, H. et al. (1993). Phosphorylation of the L-type calcium channel beta subunit is involved in beta-adrenergic signal transduction in canine myocardium. FEBS Lett., 335, 2, 217-222,

Hagiwara, N. et al. (1988). Contribution of two types of calcium currents to the pacemaker potentials of rabbit sino-atrial node cells. J. Physiol, 395, 233-253,

Hagiwara, N. et al. (1992). Background current in sino-atrial node cells of the rabbit heart. J. Physiol, 448, 53-72,

Han, X. et al. (1996). Identification and properties of an ATP-sensitive K+ current in rabbit sino-atrial node pacemaker cells. J. Physiol, 490 (Pt 2), 337-350,

Haufe, V. et al. (2005). Contribution of neuronal sodium channels to the cardiac fast sodium current INa is greater in dog heart Purkinje fibers than in ventricles. Cardiovasc. Res., 65, 1, 117-127,

He, H. et al. (1997). Overexpression of the rat sarcoplasmic reticulum Ca2+ ATPase gene in the heart of transgenic mice accelerates calcium transients and cardiac relaxation. J. Clin. Invest, 100, 2, 380-389,

Hedberg, A. et al. (1980). Differential distribution of beta-1 and beta-2 adrenergic receptors in cat and guinea-pig heart. J. Pharmacol. Exp. Ther., 212, 3, 503-508,

Hibino, H. et al. (2010). Inwardly rectifying potassium channels: their structure, function, and physiological roles. Physiol Rev., 90, 1, 291-366,

Honjo, H. et al. (1996). Correlation between electrical activity and the size of rabbit sino-atrial node cells. J. Physiol, 496 (Pt 3), 795-808,

Huang, J. et al. (2008). Novel mechanism for suppression of hyperpolarization-activated cyclic nucleotide-gated pacemaker channels by receptor-like tyrosine phosphatase-alpha. J. Biol. Chem., 283, 44, 29912-29919,

Huser, J. et al. (2000). Intracellular Ca2+ release contributes to automaticity in cat atrial pacemaker cells. J. Physiol, 524 Pt 2, 415-422,

Irisawa, H. et al. (1993). Cardiac pacemaking in the sinoatrial node. Physiol Rev., 73, 1, 197-227,

Isom, L.L. et al. (1992). Primary structure and functional expression of the beta 1 subunit of the rat brain sodium channel. Science, 256, 5058, 839-842,

Isom, L.L. et al. (1995). Structure and function of the beta 2 subunit of brain sodium channels, a transmembrane glycoprotein with a CAM motif. Cell, 83, 3, 433-442,

Jackson, H.A. et al. (2007). Evolution and structural diversification of hyperpolarization-activated cyclic nucleotide-gated channel genes. Physiol Genomics, 29, 3, 231-245,

James, T.N. (2002). Structure and function of the sinus node, AV node and His bundle of the human heart: part I-structure. Prog. Cardiovasc. Dis., 45, 3, 235-267,

Joyner, R.W. & van Capelle, F.J. (1986). Propagation through electrically coupled cells. How a small SA node drives a large atrium. Biophys. J., 50, 6, 1157-1164,

Jurkiewicz, N.K. & Sanguinetti, M.C. (1993). Rate-dependent prolongation of cardiac action potentials by a methanesulfonanilide class III antiarrhythmic agent. Specific block of rapidly activating delayed rectifier K+ current by dofetilide. Circ. Res., 72, 1, 75-83,

Kashiwakura, Y. et al. (2006). Gene transfer of a synthetic pacemaker channel into the heart: a novel strategy for biological pacing. Circulation, 114, 16, 1682-1686,

Kehat, I. et al. (2004). Electromechanical integration of cardiomyocytes derived from human embryonic stem cells. Nat. Biotechnol., 22, 10, 1282-1289,

Keith, A. & Flack, M. (1907). The Form and Nature of the Muscular Connections between the Primary Divisions of the Vertebrate Heart. J. Anat. Physiol, 41, Pt 3, 172-189,

Knollmann, B.C. et al. (2004). Isoproterenol exacerbates a long QT phenotype in Kcnq1-deficient neonatal mice: possible roles for human-like Kcnq1 isoform 1 and slow delayed rectifier K+ current. J. Pharmacol. Exp. Ther., 310, 1, 311-318,

Kodama, I. et al. (1996). Regional differences in the response of the isolated sino-atrial node of the rabbit to vagal stimulation. J. Physiol, 495 (Pt 3), 785-801,

Kohl, P. et al. (2005). Electrical coupling of fibroblasts and myocytes: relevance for cardiac propagation. J. Electrocardiol., 38, 4 Suppl, 45-50,

Kohl, P. et al. (1994). Mechanosensitive fibroblasts in the sino-atrial node region of rat heart: interaction with cardiomyocytes and possible role. Exp. Physiol, 79, 6, 943-956,

Kreitner, D. (1975). Evidence for the existence of a rapid sodium channel in the membrane of rabbit sinoatrial cells. J. Mol. Cell Cardiol., 7, 9, 655-662,

Kuo, H.C. et al. (2001). A defect in the Kv channel-interacting protein 2 (KChIP2) gene leads to a complete loss of I(to) and confers susceptibility to ventricular tachycardia. Cell, 107, 6, 801-813,

Kurokawa, J. et al. (2003). Requirement of subunit expression for cAMP-mediated regulation of a heart potassium channel. Proc. Natl. Acad. Sci. U. S. A, 100, 4, 2122-2127,

Lakatta, E.G. & DiFrancesco, D. (2009). What keeps us ticking: a funny current, a calcium clock, or both? J. Mol. Cell Cardiol., 47, 2, 157-170,

Lakatta, E.G. et al. (2010). A coupled SYSTEM of intracellular Ca2+ clocks and surface membrane voltage clocks controls the timekeeping mechanism of the heart's pacemaker. Circ. Res., 106, 4, 659-673,

Lees-Miller, J.P. et al. (2003). Selective knockout of mouse ERG1 B potassium channel eliminates I(Kr) in adult ventricular myocytes and elicits episodes of abrupt sinus bradycardia. Mol. Cell Biol., 23, 6, 1856-1862,

Lei, M. & Brown, H.F. (1996). Two components of the delayed rectifier potassium current, IK, in rabbit sino-atrial node cells. Exp. Physiol, 81, 5, 725-741,

Lei, M. et al. (2002). Role of the 293b-sensitive, slowly activating delayed rectifier potassium current, i(Ks), in pacemaker activity of rabbit isolated sino-atrial node cells. Cardiovasc. Res., 53, 1, 68-79,

Lei, M. et al. (2005). Sinus node dysfunction following targeted disruption of the murine cardiac sodium channel gene Scn5a. J. Physiol, 567, Pt 2, 387-400,

Lei, M. et al. (2000). Characterisation of the transient outward K+ current in rabbit sinoatrial node cells. Cardiovasc. Res., 46, 3, 433-441,

Lei, M. et al. (2004). Requirement of neuronal- and cardiac-type sodium channels for murine sinoatrial node pacemaking. J. Physiol, 559, Pt 3, 835-848,

Levy, M.N. (1971). Sympathetic-parasympathetic interactions in the heart. Circ. Res., 29, 5, 437-445,

Li, G.R. et al. (2003). Calcium-activated transient outward chloride current and phase 1 repolarization of swine ventricular action potential. Cardiovasc. Res., 58, 1, 89-98,

Li, G.R. et al. (1996). Evidence for two components of delayed rectifier K+ current in human ventricular myocytes. Circ. Res., 78, 4, 689-696,

Lin, J.W. et al. (1998). Yotiao, a novel protein of neuromuscular junction and brain that interacts with specific splice variants of NMDA receptor subunit NR1. J. Neurosci., 18, 6, 2017-2027,

Liu, D.W. et al. (1993). Ionic bases for electrophysiological distinctions among epicardial, midmyocardial, and endocardial myocytes from the free wall of the canine left ventricle. Circ. Res., 72, 3, 671-687,

Lopatin, A.N. et al. (1994). Potassium channel block by cytoplasmic polyamines as the mechanism of intrinsic rectification. Nature, 372, 6504, 366-369,

Ludwig, A. et al. (1998). A family of hyperpolarization-activated mammalian cation channels. Nature, 393, 6685, 587-591,

Mackaay, A.J. et al. (1980). Interaction of adrenaline and acetylcholine on cardiac pacemaker function. Functional inhomogeneity of the rabbit sinus node. J. Pharmacol. Exp. Ther., 214, 2, 417-422,

Maier, S.K. et al. (2003). An unexpected requirement for brain-type sodium channels for control of heart rate in the mouse sinoatrial node. Proc. Natl. Acad. Sci. U. S. A, 100, 6, 3507-3512,

Maltsev, V.A. et al. (2006). The emergence of a general theory of the initiation and strength of the heartbeat. J. Pharmacol. Sci., 100, 5, 338-369,

Mangoni, M.E. et al. (2003). Functional role of L-type Cav1.3 Ca2+ channels in cardiac pacemaker activity. Proc. Natl. Acad. Sci. U. S. A, 100, 9, 5543-5548,

Mangoni, M.E. & Nargeot, J. (2008). Genesis and regulation of the heart automaticity. Physiol Rev., 88, 3, 919-982,

Mangoni, M.E. et al. (2006). Bradycardia and slowing of the atrioventricular conduction in mice lacking CaV3.1/alpha1G T-type calcium channels. Circ. Res., 98, 11, 1422-1430,

Marionneau, C. et al. (2005). Specific pattern of ionic channel gene expression associated with pacemaker activity in the mouse heart. J. Physiol, 562, Pt 1, 223-234,

Marx, S.O. et al. (2002). Requirement of a macromolecular signaling complex for beta adrenergic receptor modulation of the KCNQ1-KCNE1 potassium channel. Science, 295, 5554, 496-499,

Matsuda, H. et al. (1987). Ohmic conductance through the inwardly rectifying K channel and blocking by internal Mg2+. Nature, 325, 7000, 156-159,

Matsuura, H. et al. (2002). Rapidly and slowly activating components of delayed rectifier K(+) current in guinea-pig sino-atrial node pacemaker cells. J. Physiol, 540, Pt 3, 815-830,

McLerie, M. & Lopatin, A.N. (2003). Dominant-negative suppression of I(K1) in the mouse heart leads to altered cardiac excitability. J. Mol. Cell Cardiol., 35, 4, 367-378,

McRory, J.E. et al. (2001). Molecular and functional characterization of a family of rat brain T-type calcium channels. J. Biol. Chem., 276, 6, 3999-4011,

Miake, J. et al. (2002). Biological pacemaker created by gene transfer. Nature, 419, 6903, 132-133,

Mitsuiye, T. et al. (2000). Sustained inward current during pacemaker depolarization in mammalian sinoatrial node cells. Circ. Res., 87, 2, 88-91,

Morgan, K. et al. (2000). beta 3: an additional auxiliary subunit of the voltage-sensitive sodium channel that modulates channel gating with distinct kinetics. Proc. Natl. Acad. Sci. U. S. A, 97, 5, 2308-2313,

Muramatsu, H. et al. (1996). Characterization of a TTX-sensitive Na+ current in pacemaker cells isolated from rabbit sinoatrial node. Am. J. Physiol, 270, 6 Pt 2, H2108-H2119,

Nerbonne, J.M. (2000). Molecular basis of functional voltage-gated K+ channel diversity in the mammalian myocardium. J. Physiol, 525 Pt 2, 285-298,

Nerbonne, J.M. & Kass, R.S. (2005). Molecular physiology of cardiac repolarization. Physiol Rev., 85, 4, 1205-1253,

Nikmaram, M.R. et al. (2008). Characterization of the effects of ryanodine, TTX, E-4031 and 4-AP on the sinoatrial and atrioventricular nodes. Prog. Biophys. Mol. Biol., 96, 1-3, 452-464,

Noble, D. & Tsien, R.W. (1968). The kinetics and rectifier properties of the slow potassium current in cardiac Purkinje fibres. J. Physiol, 195, 1, 185-214,

Noma, A. & Irisawa, H. (1974). Electrogenic sodium pump in rabbit sinoatrial node cell. Pflugers Arch., 351, 2, 177-182,

Noma, A. & Irisawa, H. (1975). Contribution of an electrogenic sodium pump to the membrane potential in rabbit sinoatrial node cells. Pflugers Arch., 358, 4, 289-301,

Noma, A. & Irisawa, H. (1976). A time- and voltage-dependent potassium current in the rabbit sinoatrial node cell. Pflugers Arch., 366, 2-3, 251-258,

Noma, A. & Trautwein, W. (1978). Relaxation of the ACh-induced potassium current in the rabbit sinoatrial node cell. Pflugers Arch., 377, 3, 193-200,

Ono, K. & Ito, H. (1995). Role of rapidly activating delayed rectifier K+ current in sinoatrial node pacemaker activity. Am. J. Physiol, 269, 2 Pt 2, H453-H462,

Ono, K. et al. (2000). Properties of the delayed rectifier potassium current in porcine sino-atrial node cells. J. Physiol, 524, Pt 1, 51-62,

Oosthoek, P.W. et al. (1993). Immunohistochemical delineation of the conduction system. I: The sinoatrial node. Circ. Res., 73, 3, 473-481,

Opthof, T. (2007). Embryological development of pacemaker hierarchy and membrane currents related to the function of the adult sinus node: implications for autonomic modulation of biopacemakers. Med. Biol. Eng Comput., 45, 2, 119-132,

Opthof, T. (1988). The mammalian sinoatrial node. Cardiovasc. Drugs Ther., 1, 6, 573-597,

Opthof, T. (2000). The normal range and determinants of the intrinsic heart rate in man. Cardiovasc. Res., 45, 1, 177-184,

Papadatos, G.A. et al. (2002). Slowed conduction and ventricular tachycardia after targeted disruption of the cardiac sodium channel gene Scn5a. Proc. Natl. Acad. Sci. U. S. A, 99, 9, 6210-6215,

Perez-Reyes, E. (1999). Three for T: molecular analysis of the low voltage-activated calcium channel family. Cell Mol. Life Sci., 56, 7-8, 660-669,

Peroz, D. et al. (2009). LQT1-associated mutations increase KCNQ1 proteasomal degradation independently of Derlin-1. J. Biol. Chem., 284, 8, 5250-5256,

Plaster, N.M. et al. (2001). Mutations in Kir2.1 cause the developmental and episodic electrical phenotypes of Andersen's syndrome. Cell, 105, 4, 511-519,

Plotnikov, A.N. et al. (2008). HCN212-channel biological pacemakers manifesting ventricular tachyarrhythmias are responsive to treatment with I(f) blockade. Heart Rhythm., 5, 2, 282-288,

Potapova, I. et al. (2004). Human mesenchymal stem cells as a gene delivery system to create cardiac pacemakers. Circ. Res., 94, 7, 952-959,

Protas, L. et al. (2010). Age-dependent changes in Na current magnitude and TTX-sensitivity in the canine sinoatrial node. J. Mol. Cell Cardiol., 48, 1, 172-180,

Qu, J. et al. (2002). Functional comparison of HCN isoforms expressed in ventricular and HEK 293 cells. Pflugers Arch., 444, 5, 597-601,

Qu, J. et al. (2001). HCN2 overexpression in newborn and adult ventricular myocytes: distinct effects on gating and excitability. Circ. Res., 89, 1, E8-14,

Qu, J. et al. (2003). Expression and function of a biological pacemaker in canine heart. Circulation, 107, 8, 1106-1109,

Radicke, S. et al. (2005). Expression and function of dipeptidyl-aminopeptidase-like protein 6 as a putative beta-subunit of human cardiac transient outward current encoded by Kv4.3. J. Physiol, 565, Pt 3, 751-756,

Ridley, J.M. et al. (2003). Inhibition of HERG K+ current and prolongation of the guinea-pig ventricular action potential by 4-aminopyridine. J. Physiol, 549, Pt 3, 667-672,

Roepke, T.K. et al. (2008). Targeted deletion of kcne2 impairs ventricular repolarization via disruption of I(K,slow1) and I(to,f). FASEB J., 22, 10, 3648-3660,

Ruhparwar, A. et al. (2010). Adenylate-Cyclase VI transforms ventricular cardiomyocytes into biological pacemaker cells. Tissue Eng Part A, 16, 6, 1867-1872,

Ruhparwar, A. et al. (2002). Transplanted fetal cardiomyocytes as cardiac pacemaker. Eur. J. Cardiothorac. Surg., 21, 5, 853-857,

Sakai, R. et al. (1996). Sodium--potassium pump current in rabbit sino-atrial node cells. J. Physiol, 490 (Pt 1), 51-62,

Sanguinetti, M.C. et al. (1996). Coassembly of K(V)LQT1 and minK (IsK) proteins to form cardiac I(Ks) potassium channel. Nature, 384, 6604, 80-83,

Sanguinetti, M.C. et al. (1995). A mechanistic link between an inherited and an acquired cardiac arrhythmia: HERG encodes the IKr potassium channel. Cell, 81, 2, 299-307,

Sanguinetti, M.C. & Jurkiewicz, N.K. (1990). Two components of cardiac delayed rectifier K+ current. Differential sensitivity to block by class III antiarrhythmic agents. J. Gen. Physiol, 96, 1, 195-215,

Sanguinetti, M.C. et al. (1991). Isoproterenol antagonizes prolongation of refractory period by the class III antiarrhythmic agent E-4031 in guinea pig myocytes. Mechanism of action. Circ. Res., 68, 1, 77-84,

Satoh, H. (2003). Taurine on sino-atrial nodal cells: Ca2+-dependent modulation. Adv. Exp. Med. Biol., 526, 17-23,

Shinagawa, Y. et al. (2000). The sustained inward current and inward rectifier K+ current in pacemaker cells dissociated from rat sinoatrial node. J. Physiol, 523 Pt 3, 593-605,

Singer, D. et al. (1991). The roles of the subunits in the function of the calcium channel. Science, 253, 5027, 1553-1557,

Stieber, J. et al. (2004). Pacemaker channels and sinus node arrhythmia. Trends Cardiovasc. Med., 14, 1, 23-28,

Takumi, T. et al. (1988). Cloning of a membrane protein that induces a slow voltage-gated potassium current. Science, 242, 4881, 1042-1045,

Tan, H.L. et al. (2003). Genetic control of sodium channel function. Cardiovasc. Res., 57, 4, 961-973,

Tanaka, H. et al. (2008). Species difference in the contribution of T-type calcium current to cardiac pacemaking as revealed by r(-)-efonidipine. J. Pharmacol. Sci., 107, 1, 99-102,

ten Velde, I. et al. (1995). Spatial distribution of connexin43, the major cardiac gap junction protein, visualizes the cellular network for impulse propagation from sinoatrial node to atrium. Circ. Res., 76, 5, 802-811,

Thompson, S.H. (1977). Three pharmacologically distinct potassium channels in molluscan neurones. J. Physiol, 265, 2, 465-488,

Toyoda, F. et al. (2005). Responses of the sustained inward current to autonomic agonists in guinea-pig sino-atrial node pacemaker cells. Br. J. Pharmacol., 144, 5, 660-668,

Ulens, C. & Tytgat, J. (2001). Functional heteromerization of HCN1 and HCN2 pacemaker channels. J. Biol. Chem., 276, 9, 6069-6072,

van Ginneken, A.C. & Giles, W. (1991). Voltage clamp measurements of the hyperpolarization-activated inward current I(f) in single cells from rabbit sino-atrial node. J. Physiol, 434, 57-83,

Vassort, G. & Alvarez, J. (1994). Cardiac T-type calcium current: pharmacology and roles in cardiac tissues. J. Cardiovasc. Electrophysiol., 5, 4, 376-393,

Veenstra, R.D. et al. (1992). Multiple connexins confer distinct regulatory and conductance properties of gap junctions in developing heart. Circ. Res., 71, 5, 1277-1283,

Veldkamp, M.W. et al. (2003). Contribution of sodium channel mutations to bradycardia and sinus node dysfunction in LQT3 families. Circ. Res., 92, 9, 976-983,

Verheijck, E.E. et al. (1995). Effects of delayed rectifier current blockade by E-4031 on impulse generation in single sinoatrial nodal myocytes of the rabbit. Circ. Res., 76, 4, 607-615,

Verheijck, E.E. et al. (1999). Contribution of L-type Ca2+ current to electrical activity in sinoatrial nodal myocytes of rabbits. Am. J. Physiol, 276, 3 Pt 2, H1064-H1077,

Verheijck, E.E. et al. (2002). Atrio-sinus interaction demonstrated by blockade of the rapid delayed rectifier current. Circulation, 105, 7, 880-885,

Verheijck, E.E. et al. (1998). Pacemaker synchronization of electrically coupled rabbit sinoatrial node cells. J. Gen. Physiol, 111, 1, 95-112,

Verkerk, A.O. et al. (2007a). Single cells isolated from human sinoatrial node: action potentials and numerical reconstruction of pacemaker current. Conf. Proc. IEEE Eng Med. Biol. Soc., 2007, 904-907,

Verkerk, A.O. & van Ginneken, A.C. (2001). Considerations in studying the transient outward K(+) current in cells exhibiting the hyperpolarization-activated current. Cardiovasc. Res., 52, 3, 517-520,

Verkerk, A.O. et al. (2009a). Pacemaker activity of the human sinoatrial node: role of the hyperpolarization-activated current, I(f). Int. J. Cardiol., 132, 3, 318-336,

Verkerk, A.O. et al. (2003). Ionic remodeling of sinoatrial node cells by heart failure. Circulation, 108, 6, 760-766,

Verkerk, A.O. et al. (2007b). Pacemaker current (I(f)) in the human sinoatrial node. Eur. Heart J., 28, 20, 2472-2478,

Verkerk, A.O. et al. (2009b). Is sodium current present in human sinoatrial node cells? Int. J. Biol. Sci., 5, 2, 201-204,

Vinogradova, T.M. et al. (2004). Rhythmic ryanodine receptor Ca2+ releases during diastolic depolarization of sinoatrial pacemaker cells do not require membrane depolarization. Circ. Res., 94, 6, 802-809,

Wainger, B.J. et al. (2001). Molecular mechanism of cAMP modulation of HCN pacemaker channels. Nature, 411, 6839, 805-810,

Walsh, K.B. & Kass, R.S. (1988). Regulation of a heart potassium channel by protein kinase A and C. Science, 242, 4875, 67-69,

Wang, J. et al. (2009). Induced overexpression of Na+/Ca2+ exchanger transgene: altered myocyte contractility, [Ca2+]i transients, SR Ca2+ contents, and action potential duration. Am. J. Physiol Heart Circ. Physiol, 297, 2, H590-H601,

Wilders, R. et al. (1996). Model clamp and its application to synchronization of rabbit sinoatrial node cells. Am. J. Physiol, 271, 5 Pt 2, H2168-H2182,

Winslow, R.L. & Varghese, A. (1995). Modeling the Functional Role of SA Node - Atrial Interdigitation. 649-652,

Wu, J. et al. (2008). Sinus node dysfunction in ATX-II-induced in-vitro murine model of long QT3 syndrome and rescue effect of ranolazine. Prog. Biophys. Mol. Biol., 98, 2-3, 198-207,

Xiao, R.P. et al. (1999). Recent advances in cardiac beta(2)-adrenergic signal transduction. Circ. Res., 85, 11, 1092-1100,

Xiao, Y.F. & Sigg, D.C. (2007). Biological approaches to generating cardiac biopacemaker for bradycardia. Sheng Li Xue. Bao., 59, 5, 562-570,

Xu, W. & Lipscombe, D. (2001). Neuronal Ca(V)1.3alpha(1) L-type channels activate at relatively hyperpolarized membrane potentials and are incompletely inhibited by dihydropyridines. J. Neurosci., 21, 16, 5944-5951,

Xue, T. et al. (2002). Dominant-negative suppression of. Circ. Res., 90, 12, 1267-1273,

Yang, J. et al. (1993). Molecular determinants of Ca2+ selectivity and ion permeation in L-type Ca2+ channels. Nature, 366, 6451, 158-161,

Yu, F.H. et al. (2003). Sodium channel beta4, a new disulfide-linked auxiliary subunit with similarity to beta2. J. Neurosci., 23, 20, 7577-7585,

Zaritsky, J.J. et al. (2001). The consequences of disrupting cardiac inwardly rectifying K(+) current (I(K1)) as revealed by the targeted deletion of the murine Kir2.1 and Kir2.2 genes. J. Physiol, 533, Pt 3, 697-710,

Zhang, H. et al. (2001a). Gradient model versus mosaic model of the sinoatrial node. Circulation, 103, 4, 584-588,

Zhang, H. et al. (2002a). Sustained inward current and pacemaker activity of mammalian sinoatrial node. J. Cardiovasc. Electrophysiol., 13, 8, 809-812,

Zhang, M. et al. (2001b). minK-related peptide 1 associates with Kv4.2 and modulates its gating function: potential role as beta subunit of cardiac transient outward channel? Circ. Res., 88, 10, 1012-1019,

Zhang, Z. et al. (2002b). Functional Roles of Ca(v)1.3 (alpha(1D)) calcium channel in sinoatrial nodes: insight gained using gene-targeted null mutant mice. Circ. Res., 90, 9, 981-987,

Zhou, Z. & Lipsius, S.L. (1993). Na(+)-Ca2+ exchange current in latent pacemaker cells isolated from cat right atrium. J. Physiol, 466, 263-285,

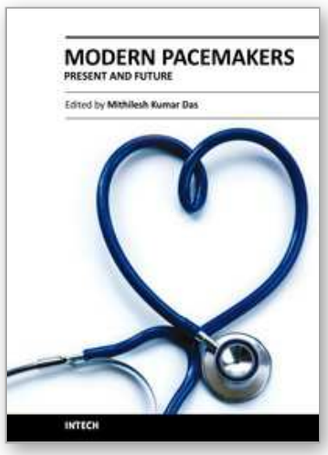

Modern Pacemakers - Present and Future

Edited by Prof. Mithilesh R Das

ISBN 978-953-307-214-2
Hard cover, 610 pages
Publisher InTech
Published online 14, February, 2011
Published in print edition February, 2011

The book focuses upon clinical as well as engineering aspects of modern cardiac pacemakers. Modern pacemaker functions, implant techniques, various complications related to implant and complications during follow-up are covered. The issue of interaction between magnetic resonance imaging and pacemakers are well discussed. Chapters are also included discussing the role of pacemakers in congenital and acquired conduction disease. Apart from pacing for bradycardia, the role of pacemakers in cardiac resynchronization therapy has been an important aspect of management of advanced heart failure. The book provides an excellent overview of implantation techniques as well as benefits and limitations of cardiac resynchronization therapy. Pacemaker follow-up with remote monitoring is getting more and more acceptance in clinical practice; therefore, chapters related to various aspects of remote monitoring are also incorporated in the book. The current aspect of cardiac pacemaker physiology and role of cardiac ion channels, as well as the present and future of biopacemakers are included to glimpse into the future management of conductions system diseases. We have also included chapters regarding gut pacemakers as well as pacemaker mechanisms of neural networks. Therefore, the book covers the entire spectrum of modern pacemaker therapy including implant techniques, device related complications, interactions, limitations, and benefits (including the role of pacing role in heart failure), as well as future prospects of cardiac pacing.

INTECH
open science | open minds

InTech Europe
University Campus STeP Ri
Slavka Krautzeka 83/A
51000 Rijeka, Croatia
Phone: +385 (51) 770 447
Fax: +385 (51) 686 166

InTech China
Unit 405, Office Block, Hotel Equatorial Shanghai
No.65, Yan An Road (West), Shanghai, 200040, China
中国上海市延安西路65号上海国际贵都大饭店办公楼405单元
Phone: +86-21-62489820
Fax: +86-21-62489821

IntechOpen

IntechOpen